Received: 19 October 2021 | Revised: 7 March 2022 | Accepted: 19 April 2022

DOI: 10.1002/eap.2684

ARTICLE

ECOLOGICAL APPLICATIONS
ECOLOGICAL SOCIETY OF AMERICA

N and P constrain C in ecosystems under climate change: Role of nutrient redistribution, accumulation, and stoichiometry

Edward B. Rastetter[1] | **Bonnie L. Kwiatkowski**[1] | **David W. Kicklighter**[1] | **Audrey Barker Plotkin**[2] | **Helene Genet**[3] | **Jesse B. Nippert**[4] | **Kimberly O'Keefe**[5] | **Steven S. Perakis**[6] | **Stephen Porder**[7] | **Sarah S. Roley**[8,9] | **Roger W. Ruess**[10] | **Jonathan R. Thompson**[2] | **William R. Wieder**[11,12] | **Kevin Wilcox**[13] | **Ruth D. Yanai**[14]

[1]The Ecosystems Center, Marine Biological Laboratory, Woods Hole, Massachusetts, USA

[2]Harvard Forest, Harvard University, Petersham, Massachusetts, USA

[3]Institute of Arctic Biology, University of Alaska Fairbanks, Fairbanks, Alaska, USA

[4]Division of Biology, Kansas State University, Manhattan, Kansas, USA

[5]Department of Biological Sciences, Saint Edward's University, Austin, Texas, USA

[6]U.S. Geological Survey, Forest and Rangeland Ecosystem Science Center, Corvallis, Oregon, USA

[7]Ecology and Evolutionary Biology, Institute for Environment and Society, Brown University, Providence, Rhode Island, USA

[8]School of the Environment, Washington State University, Richland, Washington, USA

[9]W.K. Kellogg Biological Station, Michigan State University, Hickory Corners, Michigan, USA

[10]Department of Biology and Wildlife, Institute of Arctic Biology, University of Alaska Fairbanks, Fairbanks, Alaska, USA

[11]Climate and Global Dynamics Laboratory, National Center for Atmospheric Research, Boulder, Colorado, USA

[12]Institute of Arctic and Alpine Research, University of Colorado Boulder, Boulder, Colorado, USA

[13]Department of Ecosystem Science and Management, University of Wyoming, Laramie, Wyoming, USA

[14]Department of Sustainable Resources Management, SUNY College of Environmental Science and Forestry, Syracuse, New York, USA

Correspondence
Edward B. Rastetter
Email: erastetter@mbl.edu

Funding information
DOE, Grant/Award Number: DESC0019037; National Science Foundation, Grant/Award Numbers: 1636476, 1637459, 1637653, 1637685, 1637686, 1651722, 1754126, 1832042, 1832210, 2025755, 2025849, 2220863; U.S. Forest Service, Grant/Award Number: 2019-67019-29464

Handling Editor: Yude Pan

Abstract

We use the Multiple Element Limitation (MEL) model to examine responses of 12 ecosystems to elevated carbon dioxide (CO_2), warming, and 20% decreases or increases in precipitation. Ecosystems respond synergistically to elevated CO_2, warming, and decreased precipitation combined because higher water-use efficiency with elevated CO_2 and higher fertility with warming compensate for responses to drought. Response to elevated CO_2, warming, and increased precipitation combined is additive. We analyze changes in ecosystem carbon (C) based on four nitrogen (N) and four phosphorus (P) attribution factors: (1) changes in total ecosystem N and P, (2) changes in N and P

distribution between vegetation and soil, (3) changes in vegetation C:N and C:P ratios, and (4) changes in soil C:N and C:P ratios. In the combined CO_2 and climate change simulations, all ecosystems gain C. The contributions of these four attribution factors to changes in ecosystem C storage varies among ecosystems because of differences in the initial distributions of N and P between vegetation and soil and the openness of the ecosystem N and P cycles. The net transfer of N and P from soil to vegetation dominates the C response of forests. For tundra and grasslands, the C gain is also associated with increased soil C:N and C:P. In ecosystems with symbiotic N fixation, C gains resulted from N accumulation. Because of differences in N versus P cycle openness and the distribution of organic matter between vegetation and soil, changes in the N and P attribution factors do not always parallel one another. Differences among ecosystems in C-nutrient interactions and the amount of woody biomass interact to shape ecosystem C sequestration under simulated global change. We suggest that future studies quantify the openness of the N and P cycles and changes in the distribution of C, N, and P among ecosystem components, which currently limit understanding of nutrient effects on C sequestration and responses to elevated CO_2 and climate change.

KEYWORDS
carbon dioxide fertilization, carbon sequestration, carbon–nitrogen interactions, carbon–phosphorus interactions, climate change, long-term ecological research (LTER), nitrogen cycle, phosphorus cycle, terrestrial ecosystem stoichiometry

INTRODUCTION

The response of the terrestrial biosphere to elevated carbon dioxide (CO_2) and climate change integrates the responses of many individual ecosystems, each with its own controls on its response trajectory. These individual responses are constrained by the unique biogeochemical characteristics of the ecosystems, including (1) the stocks of elements such as nitrogen (N) and phosphorus (P), (2) the cycling rates of these elements within the ecosystem, (3) the openness of these element cycles (ratio of external inputs to internal cycling, Rastetter et al., 2021), and (4) the stoichiometric flexibility of vegetation and soils (Austin & Vitousek, 2012; Leakey et al., 2012). Meta-analyses suggest that nutrient turnover rates (Ollivier et al., 2011), investment in nutrient acquisition (Xiao et al., 2018), and plant tissue N:P ratios (Yuan & Chen, 2015) all change in response to changes in CO_2 and climate. However, the responses to individual climate-change components are not consistent across biomes (e.g., Silva & Anand, 2013; Xiao et al., 2018), which presents significant challenges to making global-scale generalizations (Wieder et al., 2015). In addition, long-term responses of ecosystems to changes in CO_2 and climate are difficult to assess experimentally (Rastetter, 1996) but, like the response to other types of disturbance, likely require a redistribution of N and P stocks among ecosystem components (Rastetter et al., 1992) and a resynchronization of interdependent N and P cycles (Gress et al., 2007; Rastetter et al., 2013).

Many studies have addressed biosphere responses to elevated CO_2 and climate change across various spatial and temporal scales. Global-scale land models are used to make future projections of terrestrial biogeochemical responses to climate change (Arora et al., 2020; Bastos et al., 2020; Eby et al., 2013; Lawrence et al., 2019; McGuire et al., 2018; Melillo et al., 2009; Monier et al., 2017, 2018; Reilly et al., 2012; Zhu et al., 2020). Other studies have focused on the responses of individual ecosystems using ecosystem-scale manipulations and long-term observations (e.g., Herrick & Thomas, 2001; Mack et al., 2004; Paschalis et al., 2017; Shaver et al., 2006; Shaver & Jonasson, 1999; Wieder et al., 2017; Zaehle et al., 2014). Still others have used ecosystem-scale models to make assessments for individual ecosystem types (Campbell et al., 2009; Iverson et al., 2017; Rollinson et al., 2017; Valipour et al., 2021; Wang et al., 2019; Wu et al., 2019). Each of these approaches has both advantages and drawbacks. Because of the very broad scale of the application, global models necessarily lack detail in the representation of ecosystem processes. In contrast, ecosystem manipulations, long-term observations, and ecosystem-specific models focus on individual ecosystems and therefore do not provide a

standardized approach for comparing ecosystems. Here we take an intermediate approach, much like that used by Gerten et al. (2008) and Luo et al. (2008), where the same model is applied to several ecosystems. We apply the Multiple Element Limitation (MEL) model (Rastetter et al., 1997, 2013), a mass-balance model that simulates the movement of carbon (C), N, P, and water among ecosystem components and the constraints imposed by the interactions among these resource cycles (Figure 1) to represent 12 ecosystems ranging from prairie to forest and from the arctic to the tropics. By representing this diverse range of ecosystems with the same model and applying the same climate perturbations, we can attribute differences in the simulated response to the characteristics of the ecosystems and the prevailing climate and not to the model used to simulate them.

Our primary goal is heuristic rather than predictive (Oreskes et al., 1994). That is, our focus is on assessing how differences in the distribution, throughput, cycling rates, and interactions of C, N, P, and water affect ecosystem responses to elevated CO_2, warming, and increases or decreases in precipitation. In accordance with this heuristic goal, we examine these responses using the same simulated changes in CO_2 and temperature and the same relative changes in precipitation across all ecosystems. This standardized perturbation approach allows responses to be attributed to differences among the ecosystems and their prevailing climate rather than to differences in the perturbations to the climate. Specifically, we will address the following questions:

1. Do ecosystems gain or lose C with elevated CO_2 and climate change?
2. To realize that change in C, do the ecosystems
   a. also gain or lose N or P?
   b. redistribute N or P between soil (low C:N and C:P) and vegetation (high C:N and C:P)?
   c. change vegetation C:N or C:P?
   d. change soil C:N or C:P?
3. Do N dynamics and P dynamics shift in parallel to accommodate changes in C?
4. Does the gain or loss of C depend on the openness of the N and P cycles (quantified as the sum of N or P inputs to the ecosystem divided by the total uptake of N or P by vegetation over a year)?
5. Do changes in N and P stocks, distribution, and vegetation and soil stoichiometry differ among types of ecosystems?

METHODS

Model

We use the Multiple Element Limitation (MEL) model, which has been applied to study the recovery of northern

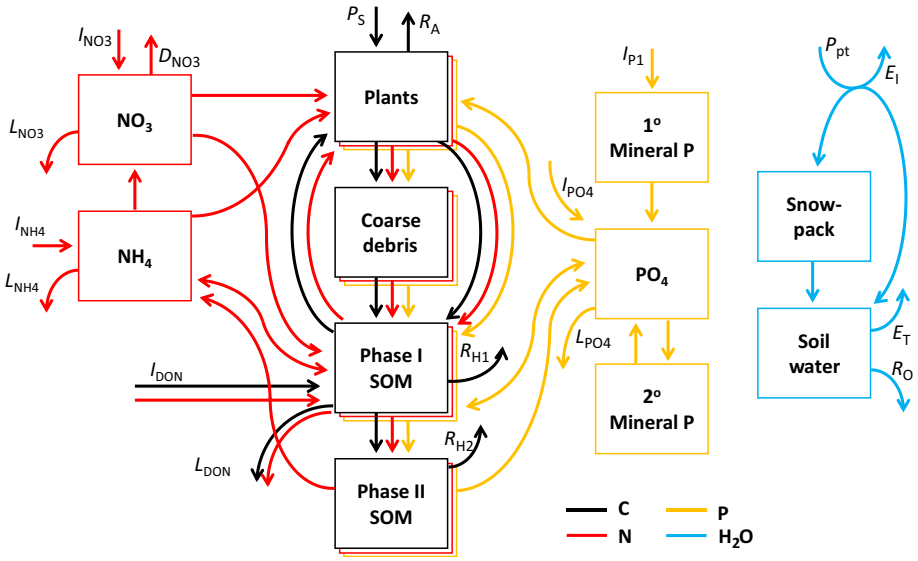

FIGURE 1 Diagram depicting the stocks and fluxes of carbon (C), nitrogen (N), phosphorus (P), and water (H_2O) represented in the Multiple Element Limitation (MEL) model. SOM is soil organic matter. For simplicity, only input and loss fluxes are labeled: P_S, R_A, R_{H1}, and R_{H2} are photosynthesis, autotrophic respiration, heterotrophic respiration from Phase I SOM, and heterotrophic respiration from Phase II SOM. I_{NH4}, I_{NO3}, I_{DON}, I_{PO4}, and I_{P1} are inputs of ammonium (NH_4), nitrate (NO_3), dissolved organic N (DON), phosphate (PO_4), and primary P minerals. L_{NH4}, L_{NO3}, L_{DON}, L_{PO4}, and D_{NO3} are leaching losses of NH_4, NO_3, DON, and PO_4 and losses of NO_3 through denitrification. Ppt is precipitation, E_I is evaporation of intercepted precipitation, E_T is transpiration, and RO is runoff. Not represented in this figure are the run-in of water, NH_4, NO_3, DON, and PO_4, which are simulated only for arctic wet-sedge tundra (ARC-w). Values for all stocks and fluxes for all 12 ecosystems are presented in Table 1.

hardwood forests from harvest (Rastetter et al., 2013) and the recovery of arctic tundra both from thermokarst mass wasting (Pearce et al., 2015) and from tundra fire (Jiang et al., 2015). The model simulates changes in C, N, and P stocks in and fluxes among plant biomass, Phase I and Phase II (Melillo et al., 1989) soil organic matter (SOM), detritus, and inorganic nutrients as well as changes in soil water content (Figure 1). Daily driving variables are atmospheric CO_2, maximum and minimum air temperature, precipitation, total shortwave radiation, and nutrient inputs. The full model structure is presented in Appendix S1 and the model itself is available at https://zenodo.org/record/6502583#.YmrnBNPMKUk. The MEL model couples ecosystem C, N, P, and water cycles and generates output for all stocks and fluxes on a daily time step. The differential equations that describe the mass balance for each of the simulated components of the ecosystem are solved numerically using a fourth/fifth-order Runge–Kutta integrator with a time-step size that adapts with each pass through the integrator to optimize precision and computation time (Press et al., 1986). The model is coded in Lazarus 2.0.4 (http://www.lazarus-ide.org) free Pascal and runs on a PC or Mac computer.

The model uses an aggregated representation of vegetation and soil components for the mass-balance equations (Figure 1). However, the vegetation biomass is partitioned into woody and active tissues (leaves plus fine roots) using an allometric equation that increases active tissues asymptotically toward a maximum as total biomass increases. The active tissues are further partitioned into leaves and fine roots in proportion to the total resource-acquisition effort allocated to canopy versus soil resources (described in the next paragraph). Resource requirements are assessed based on the current biomass C, N, and P relative to the sum of the stoichiometric optima for the individual tissues, which vary among leaves, wood, and fine roots. Vegetation stoichiometry is flexible, but resource-acquisition effort, respiration, and litter stoichiometry are constantly adjusted to drive the stoichiometry back toward the optimum. Microbial biomass is implicitly aggregated into the Phase I SOM. However, microbial processes respond to the stoichiometry of Phase I SOM, to the concentrations of ammonium (NH_4), nitrate (NO_3), and phosphate (PO_4) in soil solution, and to soil temperature and soil moisture. The stoichiometry of Phase I SOM is flexible, but the stoichiometry of Phase II SOM is fixed.

We use version VI of the MEL model, which has some improvements to the plant resource acquisition algorithm described in Rastetter et al. (2013) for version IV. The major modification we made to the model for the current application is a hierarchical allocation scheme for resource-acquisition effort (Rastetter & Kwiatkowski, 2020). We define effort allocated toward a particular resource as the fraction of all vegetation assets (e.g., allocation to leaf or root tissue, enzyme production, carbohydrate expenditure) that can be allocated toward the acquisition of resources from the environment. We assume that these assets increase as biomass increases and can be incrementally reallocated among resources. Effort is first allocated toward acquisition of C, N, and P based on the relative amounts needed to replace losses (litterfall and respiration) and to correct any stoichiometric imbalance. The primary allocation of N effort is then partitioned into sub-efforts allocated toward NH_4, NO_3, dissolved organic N (DON), and symbiotic N fixation based on the highest relative return of N per unit effort expended. Because PO_4 is the only available form of P represented in the model, there is no analogous sub-effort routine for P. The primary C effort is subdivided into sub-efforts allocated toward CO_2, light, and water acquisition based on the highest relative increase in photosynthesis per unit effort expended. All else being equal, resource acquisition increases monotonically both with biomass and with the effort allocated toward that resource.

Model drivers

For the calibration, we drive the model with daily maximum and minimum temperature (Figure 2; Henshaw et al., 2021), daily incoming shortwave radiation, atmospheric CO_2 concentration, daily precipitation (Figure 2; Henshaw et al., 2021), and daily deposition rates for NH_4, NO_3, PO_4, dissolved organic C (DOC), and DON. We specify a daily weathering rate for primary P minerals that is constant through the year and calculated based on the amount of primary P minerals for the specified soil type (Yang & Post, 2011) and a 4000-year turnover time (Boyle et al., 2013). For wet-sedge tundra (ARC-w) we specify daily run-in water and associated amounts of run-in NH_4, NO_3, PO_4, DOC, and DON. For this site, we set the annual amount of run-in water to five times the annual precipitation. The timing of the water run-in for ARC-w is the same as the runoff simulated for tussock tundra (ARC-t). The amounts of NH_4, NO_3, PO_4, DOC, and DON in the run-in are set based on their respective average annual concentrations in the simulations of leaching losses for tussock tundra at steady state. Site descriptions with drivers and links to data sources are in Appendix S2.

Calibration

We calibrate the model to ecosystems with mature vegetation and well-developed soils so we can assume a

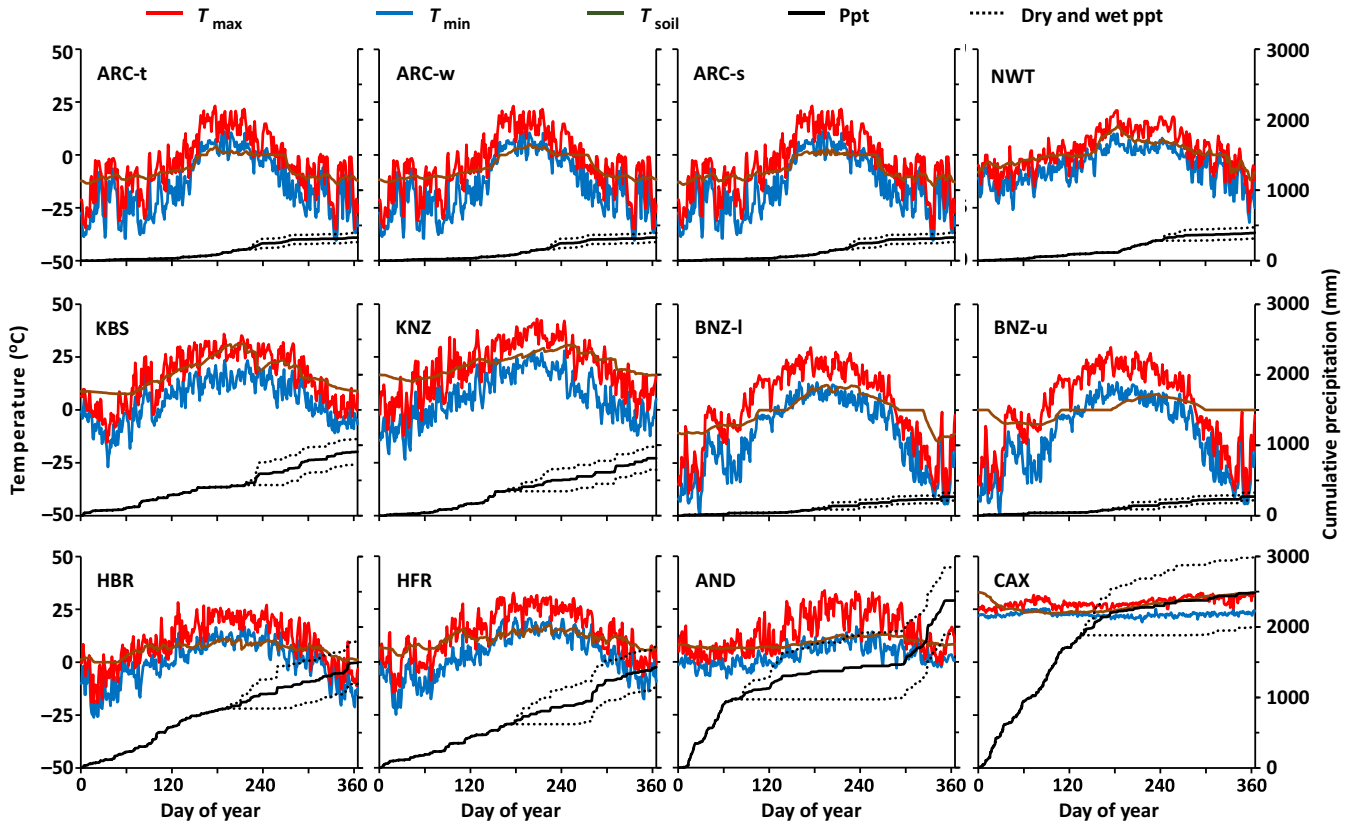

FIGURE 2 Daily maximum (T_{max}) and minimum air temperature (T_{min}) and annual cumulative precipitation used to calibrate the model to each site. Also shown is the simulated soil temperature for each site. The same climate data are used to calibrate all three arctic sites (arctic tussock tundra [ARC-t], arctic wet-sedge tundra [ARC-w], and arctic shrub tundra [ARC-s]). Similarly, the same climate data are used to calibrate the two boreal sites (boreal upland [BNZ-u] and boreal lowland [BNZ-l] black spruce forest). For arctic wet-sedge tundra (ARC-w), we assume water run-in from the surrounding watershed equivalent to five times the annual precipitation. The timing of this run-in is the same as the runoff from the arctic tussock (ARC-t). Dotted black lines are the cumulative precipitation for simulations with 20% decrease and 20% increase in annual precipitation. Ecosystems are identified in Table 1.

steady state. This steady-state assumption clearly ignores responses to climate change already underway in these ecosystems. However, the assumption effectively increases the degrees of freedom for calibration by a factor of 2 or 3 because we can assume, for example, that plant uptake, litter losses, and net mineralization of nutrients are all equal and that ecosystem inputs equal outputs. With the gaps in data for most ecosystems, this assumption helps make this analysis feasible. It also limits us to a heuristic, rather than predictive, analysis. We also recognize that by making this steady state assumption that we are ignoring biomass accumulation following infrequent disturbances like fire and erosive events that alter soil properties, both of which can be important in some of these biomes. The exceptions to this undisturbed, steady-state approach are the two prairie sites, where we also assume a steady state but with annual burning. We specify the steady-state values for all organic C, N, and P stocks and for most of the fluxes and then iteratively adjust the rate parameters for the processes until the annual cumulative C, N, P, and water fluxes match specified annual gross flux values (Table 1). We allow soil water, NH_4, NO_3, and PO_4, as well as the resource-acquisition sub-efforts for CO_2, light, water, NH_4, NO_3, DON, and symbiotic N fixation to self-adjust during the calibration.

To constrain the primary efforts of C, N, and P acquisition, we assume that the ratio of aboveground (light + CO_2) to belowground (N + P + water) effort is the same as the leaf-to-fine-root biomass ratio. This proportionality of canopy and soil resource acquisition efforts to leaf and fine-root biomass does not make resource acquisition proportional to leaf or fine-root biomass. Because of the fast turnover of nutrients in soil solution, nutrient uptake is more closely related to net mineralization than root biomass and the rates of canopy resource acquisition depend on the interactions among Beer's Law and the relative availability of CO_2 and water. The allocation of primary effort in the model helps maintain the stoichiometric balance but is not necessarily proportional to the acquisition of individual resources. To impose the specified leaf-to-fine-root biomass ratio in the calibration, the

TABLE 1 Characteristics of the 12 ecosystems in this analysis.

Characteristic	ARC-t[a]	ARC-w[b]	ARC-s[c]	NWT[d]	KBS[e]	KNZ[f]	BNZ-l[g]	BNZ-u[h]	HBR[i]	HFR[j]	AND[k]	CAX[l]
Site characteristic												
Latitude (N)	68° 38′	68° 38′	68° 27′	40° 03′	42° 24′	39° 05′	64° 45′	64° 45′	43° 57′	42° 32′	44° 14′	−1° 48′
Longitude (W)	−149° 37′	−149° 35′	−149° 22′	−105° 37′	−85° 24′	−96° 35′	−148° 18′	−148° 18′	−71° 44′	−72° 11′	−122° 10′	−51° 26′
Elevation (m)	750	745	803	3744	274	387	400	460	530	335	768	30
Mean shortwave (MJ m^{-2} day^{-1})	9.3	9.3	9.3	15.1	13.4	16.1	8.0	8.0	10.2	12.5	11.6	16.5
Mean annual temperature (°C)	−9	−9	−9	−2	10	13	−5	−5	4	8	9	25
Mean growing-season temperature (°C)	9	9	9	7	19	25	14	14	13	17	11	25
Mean annual precipitation (mm $year^{-1}$)	328	328	328	396	907	814	272	272	1496	1426	2370	2487
Soil type	Histosol	Histosol	Histosol	Inceptisol	Alfisol	Mollisol	Histosol	Inceptisol	Inceptisol	Inceptisol	Andisol	Oxisol
Field capacity (mm)	79	110	61	90	284	400	96	150	72	72	255	875
Wilting point (mm)	44	60	34	51	110	150	32	50	24	24	119	575
Soil depth (mm)	350	400	270	300	1000	1000	640	1000	479	479	796	2500
LAI (m^2 m^{-2})	1.3	0.7	1.5	1.9	3.0	3.4	1.3	2.1	5.5	3.4	7.6	4.8
N openness (unitless)[m]	0.0161	0.0244	0.0065	0.2614	0.1117	0.1316	0.0751	0.0377	0.0614	0.0696	0.0409	0.0236
P openness (unitless)[m]	0.0156	0.0547	0.0086	0.0516	0.0097	0.0312	0.0129	0.0063	0.0081	0.0073	0.0422	0.0035
C stocks[n]												
Plant C	759	567	1595	363	1526	1139	3868	6405	12006	14653	41372	25901
Detritus C	389	471	268	212	5	75	67	67	1310	2070	10218	1579
Phase I soil C	3341	5683	3245	1922	2243	2472	6047	3378	4302	3510	2443	4686
Phase II soil C	8710	14643	8433	5124	6190	6479	15624	8713	11332	9253	6300	12168
N stocks[n]												
Plant N	13.4	12.4	35.8	6.1	26.3	16.0	18.4	25.2	83.4	126.3	77.7	163.0
Detritus N	7.2	12.6	6.6	5.4	0.13	1.9	0.1	0.1	5.4	9.1	18.7	10.4
Phase I soil N	80.5	230.8	127.4	87.5	121.5	101	132.6	75.2	170.8	116.1	50.9	190.7
Phase II soil N	313.3	1087.9	599.9	436.9	771.5	629.2	597.5	331.9	629.0	468.8	347.2	1012.9
NH_4	0.038	0.081	0.071	1.408	2.941	0.781	11.263	6.644	0.288	0.333	0.327	1.442
NO_3	0.009	0.001	0.003	0.256	0.399	0.104	0.297	0.128	0.010	0.010	0.007	2.429
P stocks[n]												
Plant P	1.30	1.43	3.28	0.65	2.32	1.38	2.76	3.80	9.74	12.65	11.79	18.65
Detritus P	0.81	2.16	0.62	0.54	0.01	0.10	0.0066	0.0066	0.58	0.91	4.41	0.63
Phase I soil P	8.10	23.08	12.77	8.78	12.26	10.04	13.26	7.53	17.26	11.62	5.04	19.30
Phase II soil P	31.33	108.79	59.99	43.69	77.15	62.92	59.75	33.19	62.90	46.88	34.72	101.29
Primary P	9.5	31.7	17.5	21.6	28.8	106.9	17.6	16.7	17.1	24.1	34.6	3.8
Secondary P	6.0	22.0	12.0	9.0	17.0	18.0	12.0	7.0	21.0	11.0	22.0	75.0
PO_4	0.0406	0.0275	0.0426	0.5621	0.4762	1.4305	0.7755	0.3966	0.0422	0.0512	0.2108	0.2335
C fluxes[n]												
DOC-input	0.232	0.232	0.232	0.444	2.446	2.199	1.194	1.194	1.051	1.001	1.852	4.813
Net DOC run-in	0	9.32	0	0	0	0	0.00	0	0	0	0	0
Plant DOC uptake	4.42	3.37	12.77	3.51	12.02	13.47	7.41	14.59	0	0	0	0
GPP	409	193	741	412	879	1112	588	1113	947	1323	1076	2109
NPP	204	96	371	206	439	556	294	556	473	662	538	1055
Plant fire loss	0	0	0	0	12	4	0	0	0	0	0	0

(Continues)

TABLE 1 (Continued)

Characteristic	ARC-t[a]	ARC-w[b]	ARC-s[c]	NWT[d]	KBS[e]	KNZ[f]	BNZ-l[g]	BNZ-u[h]	HBR[i]	HFR[j]	AND[k]	CAX[l]
Litter C fine	187.8	90.7	302.6	189.5	223.2	406.1	288.4	555.1	342.0	454.0	301.6	647.1
Litter C coarse	20.9	9.0	80.8	20.0	216.2	159.2	13.0	16.0	131.3	207.6	236.5	407.5
Litter fire loss	0	0	0	0	23	89	0	0	0	0	0	0
Phase I respiration	160	81	314	157	357	404	226	435	365	512	479	932
Phase II respiration	42.7	13.4	54.9	28.9	35.2	48.2	54.9	108.5	101.2	139.7	52.2	77.2
DOC Leaching	2.1	11.3	2.1	20.7	15.3	12.4	14.0	14.0	8.2	10.4	8.5	50.4
N fluxes[n]												
NH_4 input	0.015	0.015	0.015	0.138	0.389	0.475	0.126	0.126	0.236	0.559	0.041	0.125
NO_3 input	0.020	0.020	0.020	0.181	0.389	0.523	0.055	0.055	0.462	0.301	0.057	0.108
Fire NO_3 input	0	0	0	0	0.758	1.874	0	0	0	0	0	0
DON input	0.019	0.019	0.019	0.921	0.242	0.342	0.097	0.097	0.131	0.125	0.074	0.233
Net NH_4 run-in	0	0.00819	0	0	0	0	0.000	0	0	0	0	0
Net NO_3 run-in	0	0.0241	0	0	0	0	0.0000	0	0	0	0	0
Net DON run-in	0	0.608	0	0	0	0	0.00	0	0	0	0	0
Symbiotic N fixation	0	0	0	0.18	1	0	0.083	0.083	0	0	0	1.62
Non-symbiotic N fixation	0.0907	0.0859	0.0909	0.0007	0.2500	0.2507	0.603	0.603	0.127	0.127	0.450	1.6201
Plant NH_4 uptake	1.60	1.30	4.22	1.56	4.37	4.86	1.69	3.42	10.4	10.9	4.15	9.61
Plant NO_3 uptake	0.56	0	0.57	2.23	1.52	1.68	0	0	3.09	3.24	0.049	10.08
Plant DON uptake	1.19	0.91	3.45	0.949	3.25	3.64	2.00	3.94	0	0	0	0
Plant fire loss	0	0	0	0	0.406	0.143	0	0	0	0	0	0
Litter N fine	2.97	1.97	6.24	4.42	3.90	5.98	3.76	7.4	13.0	13.2	3.77	18.6
Litter N coarse	0.388	0.241	2.00	0.505	5.82	4.06	0.023	0.028	0.545	0.917	0.432	2.67
Litter fire loss	0	0	0	0	0.570	2.27	0	0	0	0	0	0
NH_4 immobilization	6.96	2.56	16.6	12.9	20.6	23.2	5.30	11.5	49.5	52.0	14.4	73.3
NO_3 immobilization	1.68	0.0400	2.60	2.29	2.90	3.08	1.47	2.16	4.50	4.61	2.42	5.47
Phase I N mineralization	9.24	2.88	20.0	16.3	24.5	25.5	6.24	12.8	61.7	63.3	18.1	92.3
Phase II N mineralization	1.53	0.995	3.90	2.46	4.39	4.68	2.10	4.13	5.62	7.08	2.88	6.43
NH_4 leaching	0.00183	0.0352	0.00445	0.0216	0.01841	0.00620	0.036	0.0382	0.0201	0.0263	0.0229	0.00726
NO_3 leaching	0.00540	0.0044	0.00310	0.0494	0.0344	0.0381	0.0125	0.01000	0.00796	0.00955	0.00620	0.167
DON leaching	0.137	0.741	0.137	1.35	1.00	0.81	0.91	0.915	0.533	0.681	0.553	3.29
Nitrification	2.23	0	3.16	4.39	4.30	2.60	1.43	2.12	7.53	7.95	2.46	15.9
Denitrification	0	0	0	0	1.00	0.2	0.0029	0	0.395	0.395	0.04	0.242
P fluxes[n]												
PO_4 input	0.002	0.002	0.002	0.02	0.0008	0.0007	0.0017	0.0017	0.0035	0.0043	0.03	0.0023
Fire PO_4 input	0	0	0	0	0.0847	0.1259	0	0	0	0	0	0
NET PO_4 run-in	0	0.0203	0	0	0	0	0.0000	0	0	0	0	0
Primary P weathering	0.0024	0.0079	0.0044	0.0054	0.0072	0.0267	0.0044	0.0042	0.0043	0.0060	0.0087	0.0009
Secondary P weathering	0.0015	0.0055	0.003	0.0023	0.0042	0.0045	0.0030	0.0017	0.0053	0.0028	0.0055	0.0187
Plant PO_4 uptake	0.283	0.181	0.742	0.492	0.826	0.880	0.472	0.93	0.962	1.42	0.916	0.920
Plant fire loss	0	0	0	0	0.0277	0.00960	0	0	0	0	0	0
Litter P fine	0.239	0.140	0.554	0.442	0.188	0.663	0.471	0.93	0.904	1.32	0.814	0.756
Litter P coarse	0.0435	0.0413	0.188	0.0505	0.610	0.208	0.001299	0.001573	0.0580	0.0918	0.102	0.164
Litter fire loss	0	0	0	0	0.0570	0.1163	0	0	0	0	0	0
PO_4 immobilization	0.864	0.260	1.92	1.52	2.35	2.62	0.677	1.37	5.40	5.66	1.68	7.88

(Continues)

TABLE 1 (Continued)

Characteristic	ARC-t[a]	ARC-w[b]	ARC-s[c]	NWT[d]	KBS[e]	KNZ[f]	BNZ-l[g]	BNZ-u[h]	HBR[i]	HFR[j]	AND[k]	CAX[l]
Phase I P mineralization	0.994	0.341	2.27	1.76	2.66	2.91	0.94	1.88	5.80	6.37	2.31	8.16
Phase II P mineralization	0.153	0.0995	0.390	0.246	0.439	0.468	0.210	0.413	0.562	0.708	0.288	0.643
PO_4 leaching	0.0044	0.030	0.0064	0.0254	0.0080	0.0274	0.0061	0.0059	0.00781	0.0103	0.0387	0.00320
Secondary P formation	0.0015	0.0055	0.0030	0.0023	0.0042	0.0045	0.0030	0.0017	0.0053	0.0028	0.0055	0.0187
Water fluxes[n]												
Rain	158	158	158	259	792	768	174	174	1108	1218	1825	2482
Snow	170	170	170	137	114	47	98	98	388	208	545	0
Run-in	0	873	0	0	0	0	0	0	0	0	0	0
Interception	33	23	58	131	147	171	39	65	270	183	370	534
Transpiration	98	105	73	111	397	317	196	76	228	222	150	956
Run off/percolation	197	1838	197	154	362	326	37	131	998	1021	1850	1231

[a]Arctic LTER, North Slope, Alaska; Arctic Moist-Acidic Tussock Tundra ecosystem.
[b]Arctic LTER, North Slope, Alaska; Arctic Wet Sedge Tundra ecosystem.
[c]Arctic LTER, North Slope, Alaska; Arctic Shrub-Tundra ecosystem.
[d]Niwot Ridge LTER, Front Range, Colorado; Alpine Dry Meadow Tundra ecosystem.
[e]Kellogg Biological Station LTER, southern Michigan; Restored Tall-grass Prairie ecosystem.
[f]Konza Prairie LTER, Flint Hills, Kansas; Native Tall-grass Prairie ecosystem.
[g]Bonanza Creek LTER, Central Alaska; Boreal Lowland Black Spruce Forest ecosystem.
[h]Bonanza Creek LTER, Central Alaska; Boreal Upland Black Spruce Forest ecosystem.
[i]Hubbard Brook LTER, central New Hampshire; Northern Hard-wood Forest ecosystem.
[j]Harvard Forest LTER, central Massachusetts; Transition Oak-Maple Forest ecosystem.
[k]H. J. Andrews LTER, Cascade Range, Oregon; Temperate Coniferous Forest ecosystem.
[l]Caxiuanã National Forest, Pará, Brazil; Tropical Rainforest ecosystem.
[m]Openness is a measure of ecosystem dependance on external nutrient sources relative to internal nutrient cycling. It is quantified as the sum of all N or P inputs to the ecosystem divided by the total uptake of N or P by the vegetation over a year.
[n]Units as follows: C stocks, g C m^{-2}; N stocks, g N m^{-2}; P stocks, g P m^{-2}; C fluxes, g C m^{-2} $year^{-1}$; N fluxes, g N m^{-2} $year^{-1}$; P fluxes, g P m^{-2} $year^{-1}$; Water fluxes, mm $year^{-1}$.

rate constants for CO_2 and light acquisition are adjusted so that the acclimation routine allocates effort above ground to match the LAI specified for the calibration (Table 1). We set the primary efforts for N and P acquisition equal to one another under the assumption that the major source of these nutrients is recycling within the ecosystem and that the two cycles are synchronized at steady state (Rastetter et al., 2013). For the calibration, we assume the effort allocated toward water (C effort × water sub-effort) is proportional to an index of annual water demand divided by annual precipitation. The index of annual water demand is the sum over the year of the saturation vapor pressure at the maximum daily temperature minus the saturation vapor pressure at the minimum daily temperature (MPa).

Calibration sites

We calibrate the MEL model to 12 ecosystems, 11 of which are within the National Science Foundation (NSF) Long-Term Ecological Research (LTER) program (Table 1). These ecosystems are from a wide variety of biomes and climatic conditions ranging from prairie to forest and from the arctic to the tropics. Although we try to compile the data for each ecosystem from a single site, those data are never complete and the data that are collected are typically collected in different years with different weather conditions. We therefore supplement these site data with data from other similar sites and sometimes fill data gaps based on mass balance, assumed stoichiometric rules, or other generalized relationships (the key ecosystem properties needed for the model are listed in Table 1, seasonal patterns we use for calibration are illustrated in Figure 2, and more detailed description of sites and the data needed to parameterize the model, including sources, are in Appendix S2).

Comparison to eddy-covariance data

We calibrate all 12 of these ecosystems to the specified C, N, P, and water stocks and annual fluxes (Table 1)

under the assumption of a year-to-year steady state. The within-year dynamics are the result of the interaction of the parameterization and the daily drivers we use in this calibration but are not used to constrain the calibration. For sites where nearby eddy-covariance data are available (Bret-Harte et al., 2019; Euskirchen et al., 2014; NEON, 2021, details in Appendix S3), we compare the daily net ecosystem production (NEP) predicted by the model to eddy-covariance estimates of net ecosystem CO_2 exchange (NEE) under the assumption that negative NEE is a good approximation of NEP (Chapin et al., 2006). Because the calibration and eddy-covariance tower sites are not necessarily the same and because the weather data we use in the calibration are not necessarily derived from the eddy-covariance towers, we compare the model predictions to several years of eddy-covariance data to assess the model against the multi-year mean NEE for the ecosystem (Figure 3).

Simulations

For each of the 12 sites, we run six 100-year simulations beginning from the calibrated steady state (72 simulations total). The six simulations are (1) increasing CO_2 from 400 to 800 μmol mol^{-1}, (2) warming from current temperatures to current plus 3.5°C, (3) decreasing precipitation from 100% to 80% of the current annual rate, (4) increasing precipitation from 100% to 120% of the current annual rate, (5) doubling of CO_2, 3.5°C warming, and 20% decrease in precipitation, and (6) doubling of CO_2, 3.5°C warming, and 20% increase in precipitation. The MEL model uses an index of vapor pressure deficit (VPD) calculated from saturated vapor pressure at the daily maximum and minimum temperatures. For these simulations we use the present-day daily temperature range throughout. The VPD increases with warming because the average temperature increases, but we do not consider any additional changes in VPD associated with changes in the daily temperature range.

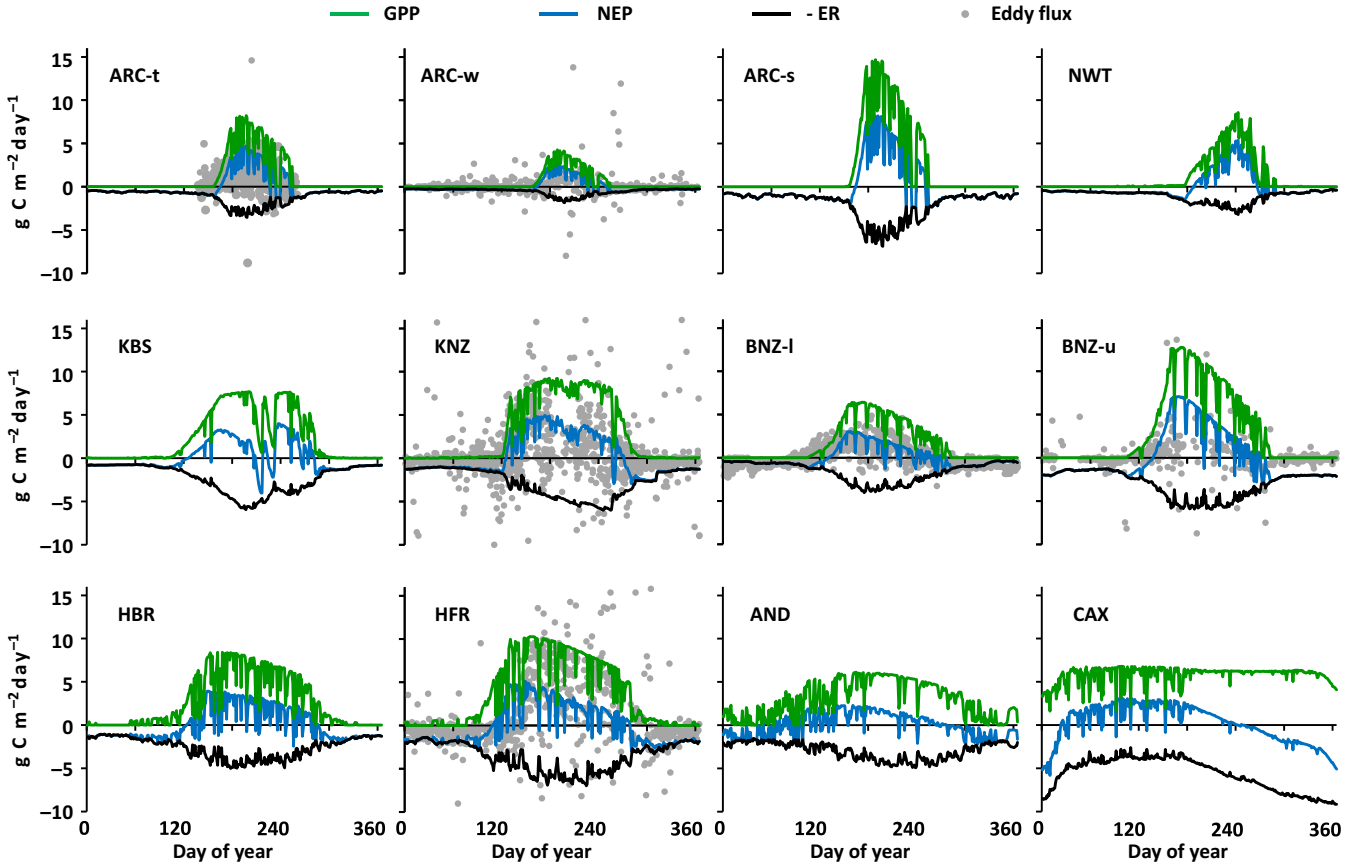

FIGURE 3 Daily gross primary production (GPP), net ecosystem production (NEP), and ecosystem respiration (ER) for the 12 ecosystems under the climate data we use to calibrate the model. Ecosystem respiration is plotted as negative values to emphasize that it is a loss from the ecosystem. Under the steady-state assumption of the calibration, NEP integrated over the year is zero. The gray dots behind the main plots are eddy covariance estimates of NEP. For the Bonanza lowland boreal forest (BNZ-l) eddy covariance data are from Euskirchen et al. (2014). For the tundra sites (ARC-t and ARC-w) eddy covariance data are from Bret-Harte et al. (2019). The remaining eddy covariance data are derived from NEON (2021) data. Ecosystems are identified in Table 1.

For these simulations, increases in CO_2 and temperature are linear over the 100 years. The temperature increase is added to the daily weather driver used to calibrate each site, thereby retaining current seasonal patterns in temperature. For decreases in precipitation, we assume drought conditions occur during the latter part of the growing season. To impose this drought, we specify a rainfall pattern for year 100 in which rainfall events closest to the end of the growing season, but prior to the time litterfall begins, are removed. The cumulative volume of the rainfall events that are removed in year 100 is equal to 20% of the initial annual rainfall (Figure 2). To meet this 20% cutoff, only a fraction of the earliest of these late-growing-season rainfall events is removed. For increased precipitation, we use an analogous approach, but double the rainfall events during the latter part of the growing season, such that 20% of the annual rainfall volume is added to the year-100 rainfall pattern (Figure 2). For the precipitation simulations, we transition linearly from the current rainfall pattern to the year-100 drought and augmented rainfall patterns. Thus, in year 1 of the simulation, a small amount is removed or added to each of the affected late-growing-season rainfall events so that the annual precipitation decreases or increases by 0.2% of the initial annual precipitation. In subsequent years the same amount is removed or added to each of the affected rainfall events until the full drought or augmented rainfall pattern is imposed in year 100. For wet-sedge tundra (ARC-w) we increase or decrease run-in water in proportion to the increase or decrease in precipitation, but we leave the annual amount of NH_4, NO_3, PO_4, DOC, and DON in the run-in unchanged (i.e., concentrations either decrease or increase as the run-in increases or decreases).

For all these simulations the drivers continue to change up through year 100 and therefore the ecosystems do not reach a new steady state. In any case, the ecosystems would require more than 100 years to establish a new steady state once the drivers no longer change because of the slow response time of soils. For the arctic and boreal sites, we simulate changes with warming in the rates of freeze and thaw of the seasonally active soil layer using a soil energy budget. However, we only account for soil down to the specified soil depth (Table 1) and therefore do not account for additional contributions to nutrient and C budgets from permafrost deeper than this depth.

Post-simulation attribution analysis

We use these simulations to determine changes in ecosystem C, N, and P stocks and fluxes in response to CO_2 and climate. We then focus our analyses on identifying nutrient and stoichiometric factors that best explain changes in total ecosystem C in response to changes in CO_2 and climate. Here we present the attribution equations for N as derived in Rastetter et al. (1992); the equations for P are analogous. In this attribution analysis, we consider five general classes of nutrient effects on gains or losses of total ecosystem C.

Changes in total ecosystem C associated with changes in total ecosystem N:

$$\Delta C_{T,\Delta N_T} = \Delta N_T (q_V f_V + q_S (1 - f_V)). \quad (1)$$

Changes in total ecosystem C associated with a change in the fraction of total ecosystem N that is in vegetation:

$$\Delta C_{T,\Delta f_V} = \Delta f_V N_T (q_V - q_S). \quad (2)$$

Changes in total ecosystem C associated with changes in vegetation C:N:

$$\Delta C_{T,\Delta q_V} = \Delta q_V N_T f_V. \quad (3)$$

Changes in total ecosystem C associated with changes in soil C:N:

$$\Delta C_{T,\Delta q_S} = \Delta q_S N_T (1 - f_V). \quad (4)$$

Changes in total ecosystem C associated with the interaction of Equations (1)–(4):

$$\begin{aligned} \Delta C_{T,int} = {} & \Delta f_V (\Delta q_V - \Delta q_S) N_T \\ & + \Delta N_T (\Delta q_V f_V + \Delta q_S (1 - f_V) + \Delta f_V (q_V - q_S)) \\ & + \Delta N_T \Delta f_V (\Delta q_V - \Delta q_S). \end{aligned} \quad (5)$$

C_T and N_T are the total C and N initially in the ecosystem (g C m^{-2} and g N m^{-2}), q_V and q_S are the initial C:N ratios of the vegetation and soil (g C g^{-1} N;), f_V is the fraction of the total ecosystem N that is initially in the vegetation, and the Δ preceding a variable indicates the change in value of that variable between initial and year 100. For this attribution analysis, soil is the sum of the C, N, or P for inorganic, detritus, and Phase I and Phase II SOM. Both primary and secondary P minerals are categorized as external to the ecosystem because of their long turnover times and consequent weak short-term interaction with the other ecosystem components. Thus, release of PO_4 from primary or secondary P minerals is treated as an input of P to the ecosystem and formation of secondary P minerals is treated as a loss of P from the ecosystem. The values calculated in Equations (1) through (5) sum to the total change in ecosystem C over the 100 years. To facilitate comparison among ecosystems

with diverse characteristics, we normalize the values from Equations (1) through (5) to percent changes in total ecosystem C by dividing by C_T and multiplying by 100.

In the initial steady state, the cycling of N and P are synchronized so that both N and P become available to support primary production in proportion to plant requirements (Rastetter et al., 2013). Superficially, the N and P cycles are similar, but there are important differences. (1) In the model, there are four potential sources of N to plants and microbes, NH_4, NO_3, DON, and N fixation, but the only direct source of P is PO_4. (2) In addition to deposition, N can enter the ecosystem through symbiotic or non-symbiotic N fixation, both of which are biologically controlled processes that are responsive, respectively, to vegetation and soil stoichiometry. In contrast, new P can enter the active ecosystem cycle only through atmospheric deposition or the slow weathering of primary or secondary P minerals, and in the model these inputs are independent of organisms or biological demand. (3) The formation and weathering of secondary P minerals serves as a long-term buffer on P availability in the ecosystem, there is no analogue of this process for N. (4) Fires volatilize a significant amount of N, but most of the P in the burned biomass and organic matter remains in the ecosystem. Because of these differences, the direct responses of the N and P cycles to climate change can differ and thereby disrupt the synchronization between N and P over the 100-year simulations. Therefore, the N-attribution factors associated with a change in ecosystem C might differ from the P-attribution factors associated with the same change in ecosystem C. To examine these interactions, we calculated correlations for each ecosystem between the N-attribution analysis and the P-attribution analysis in two ways:

1. We calculate the correlation within treatments across attribution factors to address the question "In its response to a particular treatment, do the N and P characteristics of the ecosystem change in parallel?"
2. We calculate the correlation within attribution factors across treatments to address the question "Do analogous N and P attribution factors respond in parallel across all the treatments?"

RESULTS AND DISCUSSION

Comparison to eddy flux data

For the arctic (ARC-t and ARC-w), tallgrass prairie (KNZ), and boreal lowland and upland sites (BNZ-l and BNZ-u) sites, the model and eddy-covariance estimates of NEP are consistent for the growing season, although the variance in the eddy flux data is large (Figure 3). For the winter, our model predictions are low (more negative) for KNZ and BNZ-u, which might reflect inhibition of CO_2 efflux because of frozen soil and snowpack. For the transition forest (HFR), the model estimates are low relative to the eddy-covariance data. Our assumption of a steady state is likely wrong for this site. Barford et al. (2001) and Finzi et al. (2020) estimate that this forest is accumulating C at a rate between 160 and 300 g C m^{-2} $year^{-1}$, which is consistent with the amount by which our model estimates are low. Eddy-covariance estimates can have large year-to-year variation (Barford et al., 2001; Finzi et al., 2020; both estimate 50%). Furthermore, a comparison to the net C budget only tests a small component of the overall model. Any data available for a more comprehensive test of the model had to be used for calibration (Table 1). We therefore limit ourselves to a heuristic analysis of the responses of these diverse ecosystems to elevated CO_2 and standardized changes in climate (Oreskes et al., 1994). Predictive interpretation of our results will need to wait for a more comprehensive corroboration.

Responses to elevated CO_2 alone

Over the 100-year simulations, all but one of the sites gain C with increased atmospheric CO_2 alone. The C gains are generally small as a percentage of total ecosystem C (<1%–6%, Table 2) because a large fraction of that C is in soils, especially Phase II soils, which respond slowly (over millennia). In eight of the 12 ecosystems, the response of vegetation to elevated CO_2 is much stronger (>10%, Table 2). The one ecosystem that loses C with elevated CO_2 is the lowland boreal forest (BNZ-l; Table 2). The small loss by this forest is due to the increased water-use efficiency with elevated CO_2, which results in decreased transpiration, increased runoff, and therefore increased leaching losses of N and P from the ecosystem (Figures 4 and 5). These leaching losses depend on the concentrations of NH_4, NO_3, and PO_4 in soil solution and on the dissolution of DON from soil. The losses of N and P are therefore not proportional to one another. Several other ecosystems lose N by this mechanism (ARC-t, ARC-w, ARC-s, KNZ, BNZ-u, HBR, and HFR), but the effect on C loss is compensated by increases in soil C:N ratio (ARC-t, ARC-w, ARC-s, KNZ, BNZ-u) and by the redistribution of N from soil to vegetation (BNZ-u, HBR, and HFR) so that these ecosystems gain rather than lose C. Other than the lowland boreal forest, the only ecosystem that loses P is the tallgrass prairie (KNZ), but increases in vegetation and soil C:P ratio compensate so that there is no net C loss from the ecosystem. In all five

TABLE 2 Percent change in vegetation, soil, and total-ecosystem C after 100 years in simulations of elevated CO_2, warming, decreased and increased precipitation (Ppt), alone and in combination.

Site	$2 \times CO_2 + 3.5°C$ − 20% Ppt	−20% Ppt	$2 \times CO_2$	+3.5°C	+20% Ppt	$2 \times CO_2 + 3.5°C$ + 20% Ppt
ARC-t						
Vegetation	23.38	1.38	13.59	12.21	−0.20	24.16
Soil	0.22	0.26	0.61	0.00	−0.27	−0.06
Total	1.46	0.32	1.31	0.66	−0.26	1.24
ARC-w						
Vegetation	32.25	3.65	10.62	21.88	−3.76	29.95
Soil	1.00	0.64	0.55	0.27	−0.58	0.02
Total	1.80	0.72	0.81	0.82	−0.66	0.79
ARC-s						
Vegetation	10.73	0.48	10.67	1.44	−0.04	11.22
Soil	0.78	0.16	0.77	0.13	−0.18	0.57
Total	1.90	0.19	1.88	0.28	−0.16	1.77
NWT						
Vegetation	97.22	−56.24	27.34	66.79	18.02	89.46
Soil	5.27	−17.67	4.47	2.34	3.55	4.07
Total	7.53	−18.62	5.03	3.93	3.91	6.18
KBS						
Vegetation	47.85	−34.35	17.43	−8.70	−2.77	31.14
Soil	2.08	−9.73	1.67	−1.54	0.11	0.83
Total	8.51	−13.19	3.88	−2.55	−0.29	5.09
KNZ						
Vegetation	29.20	6.27	2.07	18.77	−14.65	16.37
Soil	1.87	0.63	0.84	0.86	−3.09	0.37
Total	4.51	1.18	0.96	2.59	−4.20	1.92
BNZ-l						
Vegetation	37.91	−33.47	−1.34	−9.73	−2.68	35.61
Soil	−1.02	−3.75	−1.99	−2.73	−2.33	−3.44
Total	4.81	−8.20	−1.89	−3.78	−2.38	2.40
BNZ-u						
Vegetation	14.80	−3.31	−0.32	23.51	3.95	26.51
Soil	0.65	0.61	1.44	−0.52	−0.77	−0.34
Total	5.47	−0.73	0.84	7.67	0.84	8.81
HBR						
Vegetation	3.97	−52.43	13.27	6.71	−0.63	23.05
Soil	−0.17	0.50	−0.55	−2.18	−0.63	−3.44
Total	1.53	−21.31	5.15	1.49	−0.63	7.47
HFR						
Vegetation	12.10	−34.90	12.59	11.19	−2.68	22.15
Soil	−0.05	5.36	−1.26	−3.28	−0.80	−5.44
Total	5.96	−14.54	5.58	3.87	−1.73	8.20

(Continues)

TABLE 2 (Continued)

Site	$2 \times CO_2 + 3.5°C - 20\%$ Ppt	−20% Ppt	$2 \times CO_2$	+3.5°C	+20% Ppt	$2 \times CO_2 + 3.5°C + 20\%$ Ppt
AND						
Vegetation	12.04	−0.04	5.18	5.25	−0.82	10.65
Soil	−3.96	−0.83	0.77	−4.17	−0.31	−3.35
Total	7.00	−0.29	3.79	2.28	−0.66	6.25
CAX						
Vegetation	22.94	−17.89	11.68	−9.93	10.92	16.33
Soil	−3.67	−5.70	3.56	−3.84	1.36	3.09
Total	11.81	−12.79	8.28	−7.38	6.92	10.79

Note: Sites are identified in Table 1.

ecosystems where symbiotic N fixation is modeled explicitly (NWT, KBS, BNZ-l, BNZ-u, and CAX), elevated CO_2 increases N demand and stimulates N fixation. However, in only three of these ecosystems (NWT, KBS, and CAX) is there a resulting N accumulation and associated C gain. In the other two ecosystems (BNZ-l and BNZ-u) the N gain through N fixation is compensated by a larger increase in NH_4, NO_3, and DON leaching, resulting in a net loss of ecosystem N. For most of the tundra and grassland ecosystems (ARC-t, ARC-w, ARC-s, NWT, and KNZ), the C gain results predominantly from an increase in the C:N and C:P ratio of soil and from an input of PO_4 into the active P cycle, mostly from secondary minerals (Figures 4 and 5). For the restored prairie (KBS), the C gain also results from an increase in soil C:P, but the stimulation of symbiotic N fixation results in a large increase in ecosystem N and an associated decrease in soil C:N. For four of the forested ecosystems (HBR, HFR, AND, and CAX), the C gain is mostly in vegetation and is possible because of a net increase in the fraction of ecosystem N and P that is in vegetation (Figures 4 and 5). The upland boreal forest (BNZ-u) also gains C by a net transfer of N from soil to vegetation, but not a parallel transfer of P; instead, the C:P of the vegetation increases. The upland boreal forest (BNZ-u) also gains C because soil C:N and C:P increases.

Responses to warming alone

All but three ecosystems (KBS, BNZ-l, and CAX) gain C with 100 years of warming alone (Table 2). This C gain results from the direct stimulation of photosynthesis and N and P mineralization by warming, all of which promote plant growth. Therefore, warming in most ecosystems causes a net increase in the fraction of total ecosystem nutrient stocks that are in vegetation (Figures 4 and 5). The resulting stimulation of productivity in our simulations is stronger than the stimulation of soil respiration in most ecosystems. The increased production also enables all these ecosystems to accumulate N and P. The tropical rainforest (CAX), restored prairie (KBS), and lowland boreal forest (BNZ-l) lose C with warming. These ecosystems rely on symbiotic N fixation for 7.6% (CAX), 9.1% (KBS), and 2.2% (BNZ-l) of the N supporting annual primary production and therefore do not cycle N as tightly as the other ecosystems (i.e., a more open N cycle in that N input to the ecosystem is larger relative to internal N cycling than in the other ecosystems). Stimulation of N mineralization by warming has two effects in these ecosystems. First, the increase in available N induces a redistribution of sub-efforts among the N sources, which inhibits N fixation, resulting in a ∼30% decline in symbiotic N fixation in the tropical rainforest (CAX) and ∼60% decline in the restored prairie (KBS) and lowland boreal forest (BNZ-l). Second, the increase in mineral N increases the N losses in all three ecosystems. The net result is a loss of N from the ecosystem and, in the rainforest (CAX), a decrease in the fraction of the remaining N in vegetation. To accommodate this loss of N, the ecosystems lose P (including losses to secondary P minerals), redistribute P from vegetation to soils, and decrease the C:P of soils (Figures 4 and 5). The upland boreal forest (BNZ-u) and alpine dry meadow (NWT) also have symbiotic N fixation that declines with warming (BNZ-u by ∼20% and NWT by ∼60%). However, the stimulation of growth by warming is strong enough that these ecosystems gain C, increase N and P retention, and gain N and P.

Responses to decreased precipitation alone

The gradual decrease over 100 years in the magnitude of the rainfall events in the latter part of the growing season results in a substantial loss in vegetation biomass in half

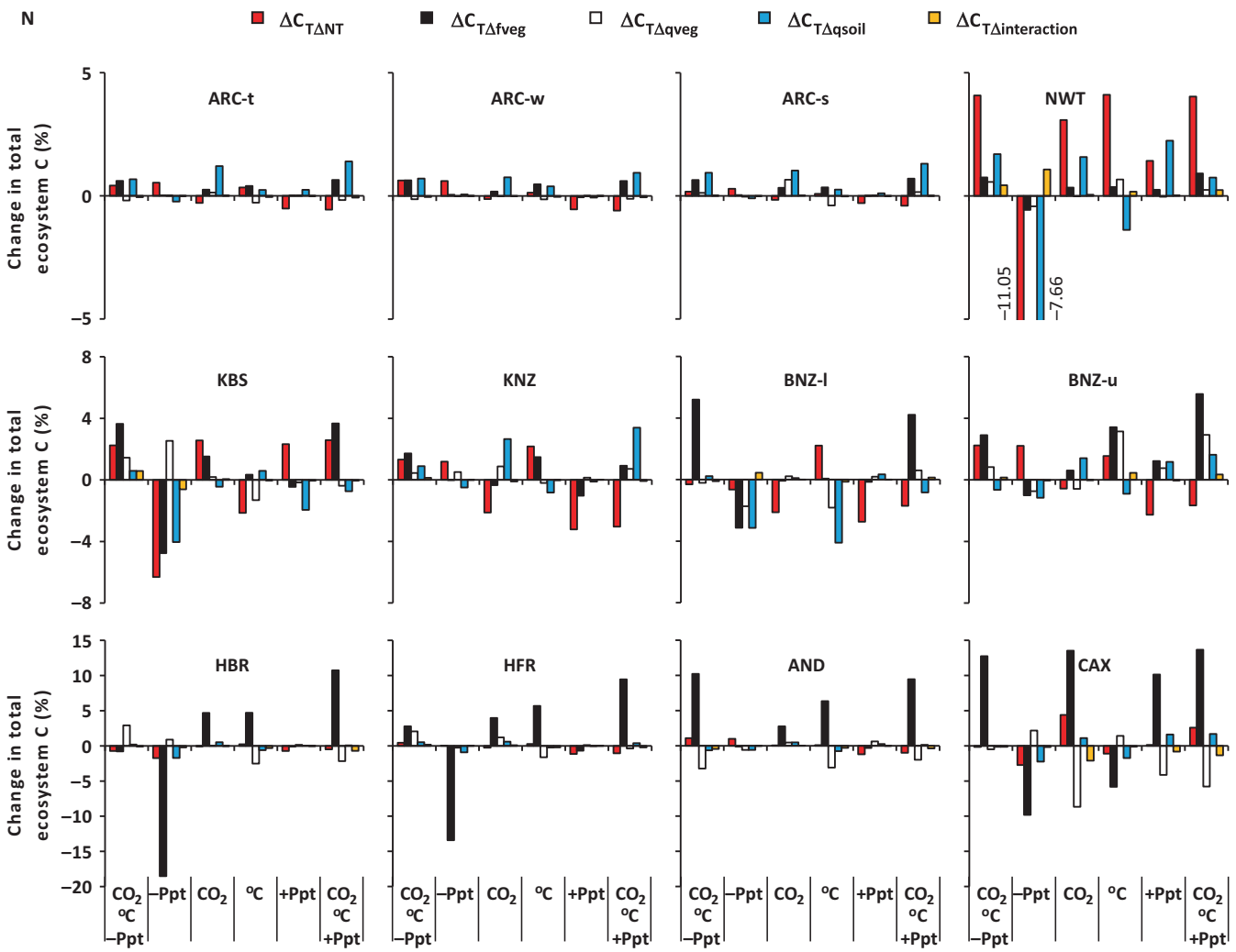

FIGURE 4 N-attribution of the percent change in total ecosystem C between initial and year-100 in response to doubled CO_2 (CO_2), 3.5°C warming (°C), and 20% decrease or increase in precipitation (−Ppt, +Ppt), alone or in combination. The changes in CO_2, temperature, and precipitation are imposed gradually as linear changes over 100 years. The five N-attribution factors (Equations 1–5) are the changes in total ecosystem C associated with (1) the changes in total ecosystem N ($\Delta C_{T\Delta NT}$), (2) changes in the fraction of total ecosystem N in vegetation ($\Delta C_{T\Delta fveg}$), (3) changes in vegetation C:N ($\Delta C_{T\Delta qveg}$), (4) changes in soil C:N ($\Delta C_{T\Delta qsoil}$), and (5) the interactions among 1–4 ($\Delta C_{T\Delta interaction}$). The sum of these five attribution factors for each treatment equals the total percent change in ecosystem C over the 100 years. These total percent changes are presented in Table 2. Ecosystems are identified in Table 1.

of the ecosystems (Figure 6 and Table 2). Of these ecosystems, some begin to lose biomass early in the simulations (NWT, KBS, BNZ-l, and CAX, Figure 6). In the others, several years of declining rainfall are required before a critical level of water limitation is reached and biomass declines (HBR, and HFR, Figure 6). Some work, especially dendroecological studies, indicate that water availability strongly regulates forest ecosystem C gain (at least in the aboveground biomass), even when water is not obviously limiting (Martin-Benito & Pederson, 2015). The drought results in losses of vegetation C that are proportionally larger than C losses from soil (if any). Thus, a decrease in the fraction of total ecosystem N and P in vegetation is a major attribution factor contributing to C loss in these six ecosystems (Figures 4 and 5). The decreased production also decreases the amount of litter production. Because litter has higher C:N and C:P ratios than the soil, the decrease in litter inputs results in a decline in the soil C:N and C:P in these six ecosystems, contributing to the total ecosystem C loss (Figures 4 and 5).

All three arctic ecosystems (ARC-t, ARC-w, ARC-s), the tallgrass prairie (KNZ), the upland boreal forest (BNZ-u), and the temperate coniferous forest (AND) gain N and P with decreased precipitation because the resulting decrease in runoff decreases N and P leaching losses (Figures 4 and 5). For all these ecosystems, the change in vegetation biomass is small (Figure 6). For the tallgrass prairie (KNZ), this nutrient gain increases

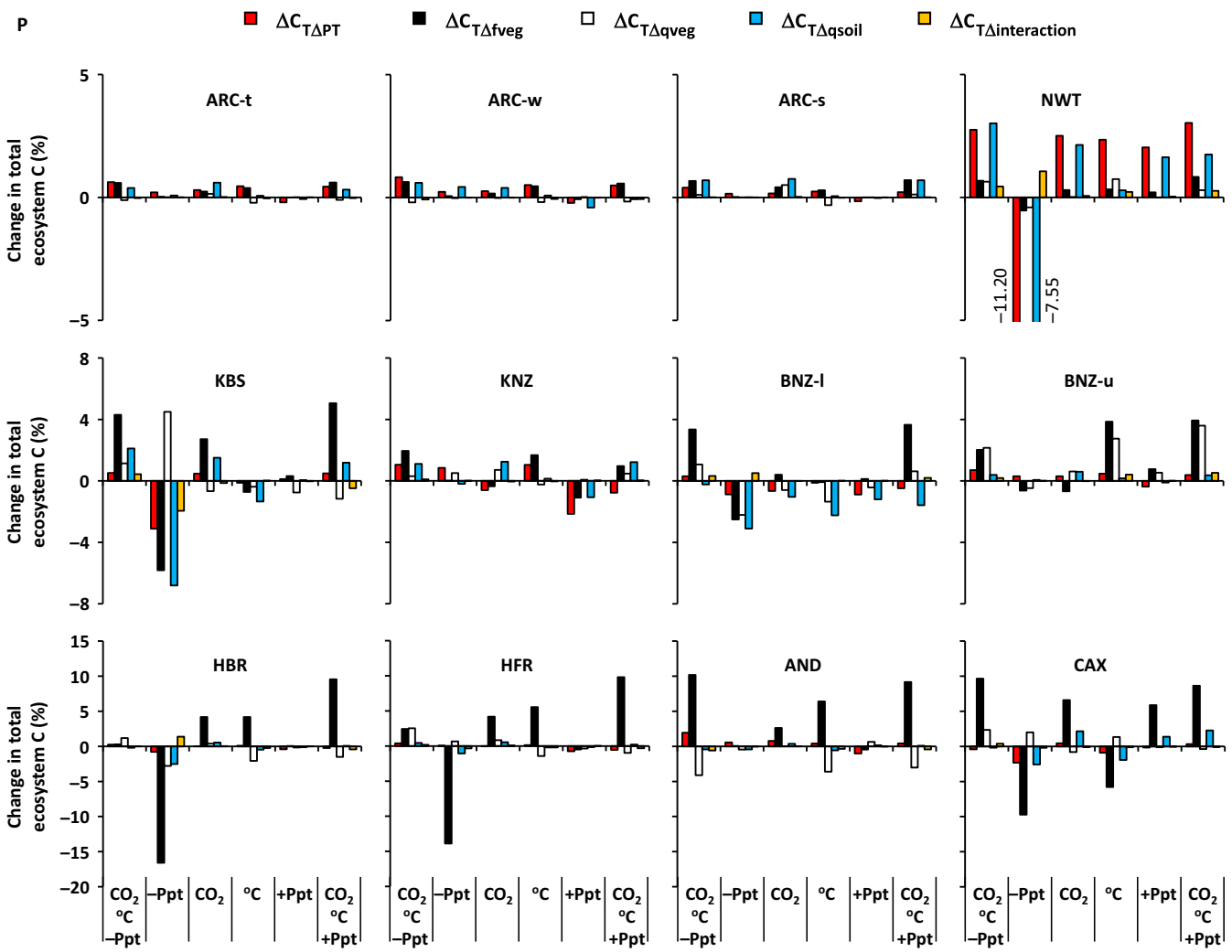

FIGURE 5 P-attribution of the percent change in total ecosystem C between initial and year-100 in response to doubled CO_2 (CO_2), 3.5°C warming (°C), and 20% decreased or increased in precipitation (−Ppt, +Ppt), alone or in combination. The changes in CO_2, temperature, and precipitation are imposed gradually as linear changes over 100 years. The five P-attribution factors (analogous to Equations 1–5, but for P) are the changes in total ecosystem C associated with (1) the changes in total ecosystem P ($\Delta C_{T\Delta PT}$), (2) changes in the fraction of total ecosystem P in vegetation ($\Delta C_{T\Delta fveg}$), (3) changes in vegetation C:P ratio ($\Delta C_{T\Delta qveg}$), (4) changes in soil C:P ratio ($\Delta C_{T\Delta qsoil}$), and (5) the interactions among 1–4 ($\Delta C_{T\Delta interaction}$). The sum of these five attribution factors for each treatment equals the total percent change in ecosystem C over the 100 years. These total percent changes are presented in Table 2. The results presented here are for the same simulations as in Figure 4. Ecosystems are identified in Table 1.

vegetation biomass for the first ~40 years of the simulation before the increasing level of drought begins to decrease biomass (Figure 6); in year 100 the biomass is nevertheless about 6% higher than the initial biomass (Table 2).

The differences in response to drought between the two boreal forests (BNZ-l and BNZ-u) and between the restored prairie (KBS) and the tallgrass prairie (KNZ) are particularly striking because each pair of ecosystems are seemingly similar. The differences in response can be traced to differences in ecosystem characteristics. For the two boreal forests, the difference can be attributed to the differences in soil depth and consequent differences in available water-holding capacity (Table 1, field capacity minus wilting point). The lower water-holding capacity of the lowland boreal forest (BNZ-l) in our calibration means that the soil cannot hold enough water to supply the water needs of the vegetation during the drought whereas the upland boreal forest (BNZ-u) soil can.

Although the tallgrass prairie (KNZ) and the restored prairie (KBS) have the same soil depth in our calibrations, the difference in soil types means that the available water-holding capacity is 44% higher in the tallgrass prairie (KNZ) than the restored prairie (KBS, Table 1). The

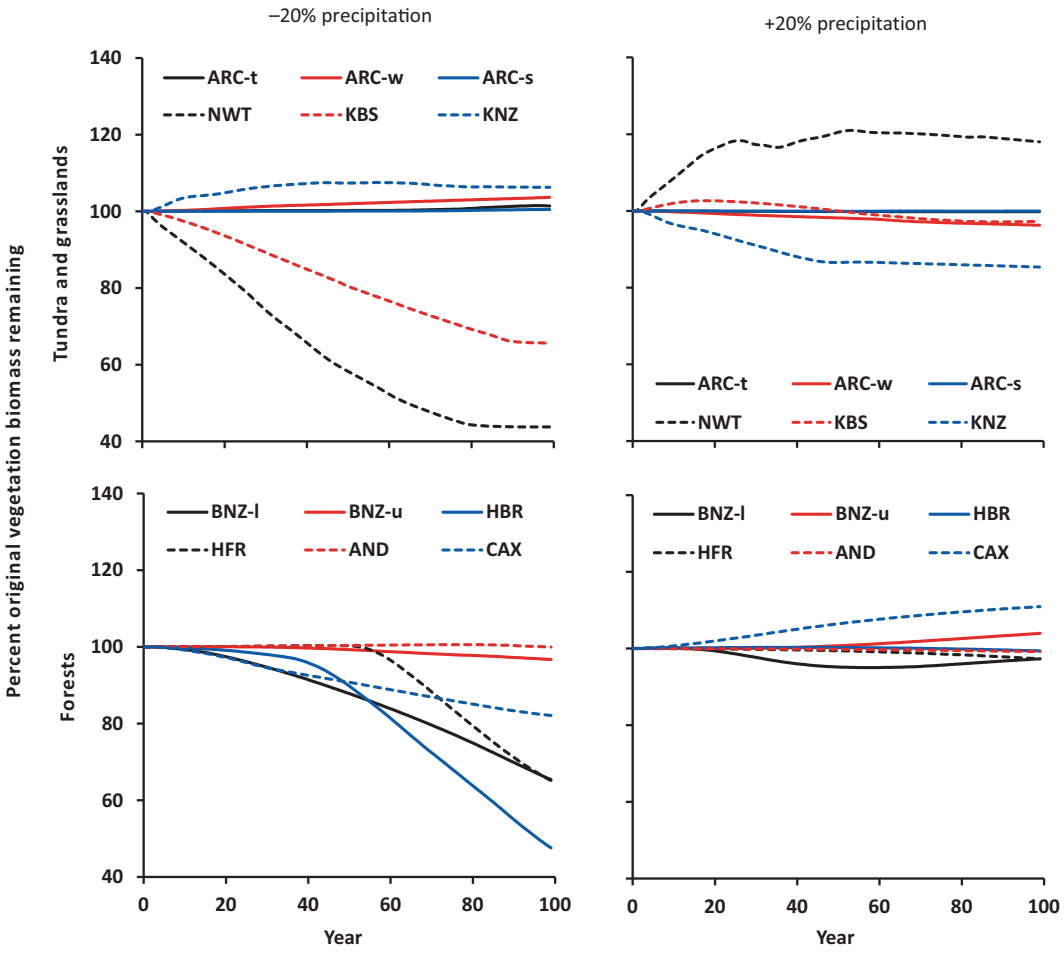

FIGURE 6 Changes in vegetation biomass in response to a gradual 20% decrease (left) and a 20% increase (right) in precipitation among tundra and grassland ecosystems (upper) and forests (lower). The decrease and increase are imposed by decreasing or increasing the intensity of rainfall events in the latter part of the growing season by successively larger amounts each year until the annual precipitation is decreased or increased by 20% by year 100. Ecosystems are identified in Table 1.

tallgrass prairie (KNZ) therefore can store more water to sustain it through a dry period. In addition, the imposed drought in the tallgrass prairie (KNZ) is immediately preceded by a wet period and the largest rainfall event of the year while the imposed drought in the restored prairie (KBS) is preceded by a dry period and the ecosystem is already in a drought before the imposed decrease in precipitation (Figure 7). Without this serendipitous large rainfall event and the high water-holding capacity of the soil at the tallgrass prairie (KNZ), it too would be more responsive to the imposed drought. Finally, the high rate of symbiotic N fixation in the restored prairie (KBS) means that it is not as responsive to the decrease in leaching losses of N with decreased precipitation. The higher N retention therefore has a stronger fertilizing effect on the tallgrass prairie (KNZ) than the restored prairie (KBS). Because of the weak response to decreased leaching losses of N and the strong drought effect, the restored prairie (KBS) loses over a third of its vegetation biomass (Figure 6). For the tallgrass prairie (KNZ), the effect of higher nutrient retention is stronger than the effect of drought, resulting in a net increase in vegetation biomass in the simulation (Figure 6).

The biomass loss because of drought is high in ecosystems with high plant water demand relative to the soil water-holding capacity. In addition, the decline in production results in less N uptake by vegetation, which can lead to inorganic N accumulation in soil that is leached out during wet periods of the year. These N losses can lead to further limitation on plant production, resulting in a positive feedback between decreased production and N loss. The N losses are strongest in ecosystems where deposition of NH_4, NO_3, and DON are high relative to the plant uptake of NH_4, NO_3, and DON. This ratio of deposition to uptake is a measure of the openness of the ecosystem N cycle (Rastetter et al., 2021). Across all 12 ecosystems, the amount of vegetation biomass remaining after 100 years of decreasing precipitation can be

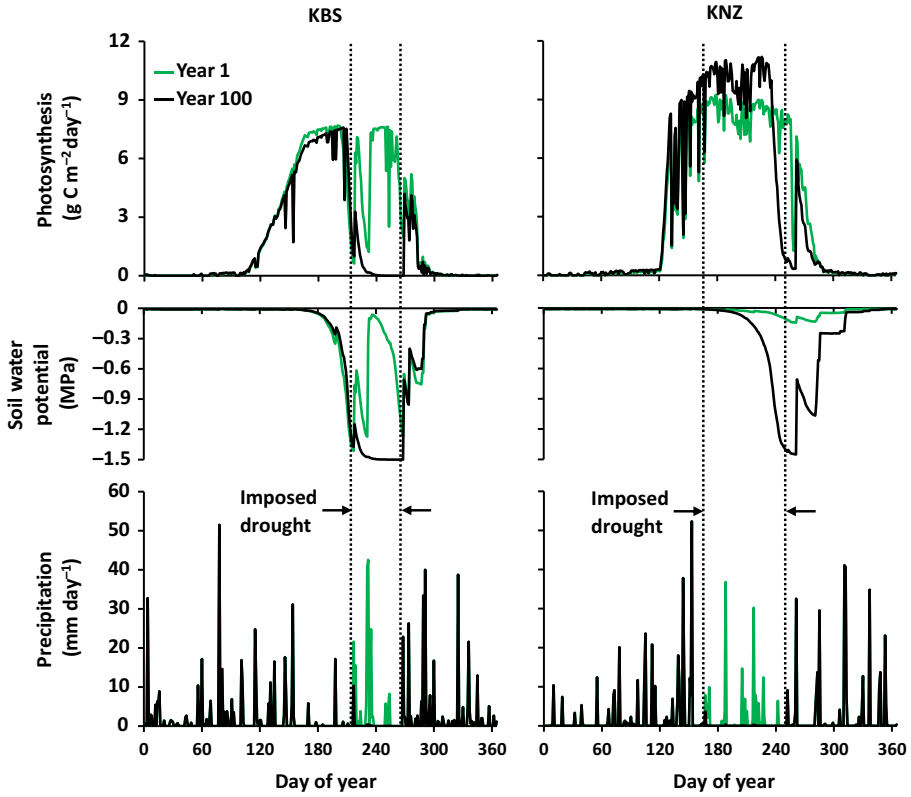

FIGURE 7 Comparison of responses of the restored prairie (KBS) and the tallgrass prairie (KNZ) to imposed drought. The intensity of the drought increased linearly between year 1 (green) and year 100 (black) until 20% of the annual precipitation is removed during the latter part of the growing season. The tallgrass prairie (KNZ) site is able to do better during the imposed drought because of the serendipitous large rainfall event just prior to the imposed drought and because of the high water-holding capacity of the soil.

predicted from water demand relative to the available water-holding capacity of the soil and from the openness of the N cycle:

$$\frac{B_{100}}{B_0} = 1.26 - 0.12\frac{E_T}{A_{\mathrm{WC}}} - 1.87\frac{T_{\mathrm{N}}}{\Omega_{\mathrm{N}}} \left(R^2 = 0.78, p < 0.001\right) \quad (6)$$

where B_0 and B_{100} are vegetation biomass at years 0 and 100 of the reduced precipitation simulation (g C m^{-2}), E_T is the annual transpiration at the calibrated steady state in year 1 (mm $year^{-1}$), A_{WC} is the available water-holding capacity of the soil (mm; Table 1 field capacity minus wilting point), T_{N} is the sum of NH_4, NO_3, and DON deposition in year 1 (g N m^{-2} $year^{-1}$), and Ω_{N} is the internal N cycling rate in year 1 (g N m^{-2} $year^{-1}$; estimated as the sum of plant N uptake of NH_4, NO_3, and DON). Although the N- and P-attribution factors are strongly correlated in the simulations of the ecosystems that lose biomass in response to decreased precipitation (NWT, KBS, BNZ-l, HBR, HFR, and CAX; Table 3), unlike the openness of the N cycle, the openness of the P cycle (ratio of P deposition plus weathering to internal P cycling) is not correlated with biomass loss.

Responses to increased precipitation alone

Increasing precipitation at the end of the growing season has less pronounced effects on vegetation biomass than decreasing precipitation (Figure 6). In the alpine dry meadow (NWT), where transpiration is high relative to the available water-holding capacity, increased precipitation increases production, symbiotic N fixation, and plant biomass. The C gain in this ecosystem is attributed to the fixation-driven increase in ecosystem N, to an increase in soil C:N and C:P resulting from the increased production and litter inputs to soil, and to an increase in ecosystem P resulting from the higher production and consequent higher P retention efficiency (Figures 4 and 5). The restored prairie (KBS) also gains N through symbiotic N fixation, but the ecosystem does not also gain P (Figures 4 and 5). Instead, N accumulates in the soil and soil C:N decreases. The net result is little net change in vegetation biomass (Figure 6). For the tropical rainforest (CAX), the increase in precipitation occurs just before the beginning of the dry season, so the soil water reserves increase and can maintain production for longer through the dry season, which allows biomass to accumulate (Figure 6). The

TABLE 3 Correlation between N- versus P-attribution factors for each ecosystem within treatments across attribution factors.

Site	$2 \times CO_2 +$ 3.5 °C − 20% Ppt	−20% Ppt	$2 \times CO_2$	+3.5 °C	+20% Ppt	$2 \times CO_2 +$ 3.5 °C + 20% Ppt
ARC-t	0.89*	0.73	0.77	0.92*	0.75	0.32
ARC-w	0.97**	0.35	0.67	0.64	0.36	−0.13
ARC-s	0.92*	0.94*	0.94*	0.88*	0.91*	0.83
NWT	0.79	1.00**	0.95*	0.94*	0.91*	0.91*
KBS	0.67	0.83	0.23	−0.62	0.06	0.74
KNZ	0.96**	0.99**	0.96**	0.82	0.89*	0.95*
BNZ-l	0.92*	0.97*	0.18	0.90*	0.28	0.94*
BNZ-u	0.56	0.68	−0.13	0.89*	0.70	0.85
HBR	0.80	0.96**	1.00**	1.00**	0.74	1.00**
HFR	0.97**	1.00**	0.99**	1.00**	0.86	1.00**
AND	0.99**	0.98**	0.93*	1.00**	0.99**	0.98**
CAX	0.96**	1.00**	0.89*	1.00**	0.95*	0.94*
Regression	$y = -0.25x + 1.41$	$y = -0.52x + 1.52$	$y = -1.00x + 1.52$	$y = -0.57x + 1.56$	$y = -0.61 + 1.38$	$y = -0.63x + 1.48$
R^2	0.17	0.32	0.60	0.45[a]	0.37	0.29
p	0.175	0.055	0.010	0.023[a]	0.035	0.071

Note: *$p < 0.05$, df = 3, **$p < 0.01$, df = 3. Regressions relate the correlations for each climate-change scenario, across sites, to the fraction of plant N uptake in the form of dissolved organic nitrogen (DON) or symbiotic N fixation. To linearize correlations for the regression, they are transformed with a modified arcsine transform (Equation 7). Sites are identified in Table 1.

[a]Restored Tall-grass Prairie (KBS) correlation removed as an outlier in regression for warming.

ecosystem C gain in the tropical rainforest (CAX) is attributed predominantly to a net transfer of N and P from soil to vegetation (Figures 4 and 5). The remaining ecosystems either change little in response to increased precipitation or lose a small amount of C because N and P are leached out of the ecosystem by increased runoff (Figures 4 and 5).

Response to multi-component climate-change simulations

All ecosystems gain C in response to the combined elevated CO_2, warming, and either increased or decreased precipitation (Table 2). The increase in water-use efficiency associated with elevated CO_2 and the increase in fertility associated with higher mineralization with warming compensates for the lower water supply in the simulations with a 20% decrease in precipitation. Thus, even those ecosystems that lose a large amount of C in the simulation with decreased precipitation alone gain C in the simulation where that decrease in precipitation is coupled with elevated CO_2 and warming.

To help assess the relative importance of the individual climate factors on the multi-component climate-change simulations, we calculate type-I regressions (Sokal & Rohlf, 1995) of percent change in total ecosystem C in multi-component versus single-component simulations; regressions combine simulations with decreased and increased precipitation (Figure 8). The response to elevated CO_2 alone dominates the response in the multi-component climate-change simulations (Figure 8a; regression near the 1:1 line). If ecosystems with symbiotic N fixation are removed from the analysis, the response to warming alone also contributes significantly to the multi-component response (Figure 8b). The responses to either decreases or increases in precipitation are not correlated to the overall responses in the combined climate-change simulations (Figure 8c). Because of the compensating effects of increased water-use efficiency with elevated CO_2 and increased fertility with warming, the interactions among elevated CO_2, warming, and decreased precipitation are strongly synergistic for the six ecosystems that lose biomass in the simulations with decreased precipitation alone (Table 2; NWT, KBS, BNZ-l, HBR, HFR, and CAX). In these six ecosystems, the multi-component response is synergistic in that the sum of the changes in ecosystem C in response to each climate component alone is negative, but the ecosystems nevertheless gain C in the multi-component simulations (Figure 8d). Luo et al. (2008) found similar synergistic interactions in their simulations of forested and the prairie ecosystems. The interactions among elevated CO_2, warming, and increased precipitation are nearly additive

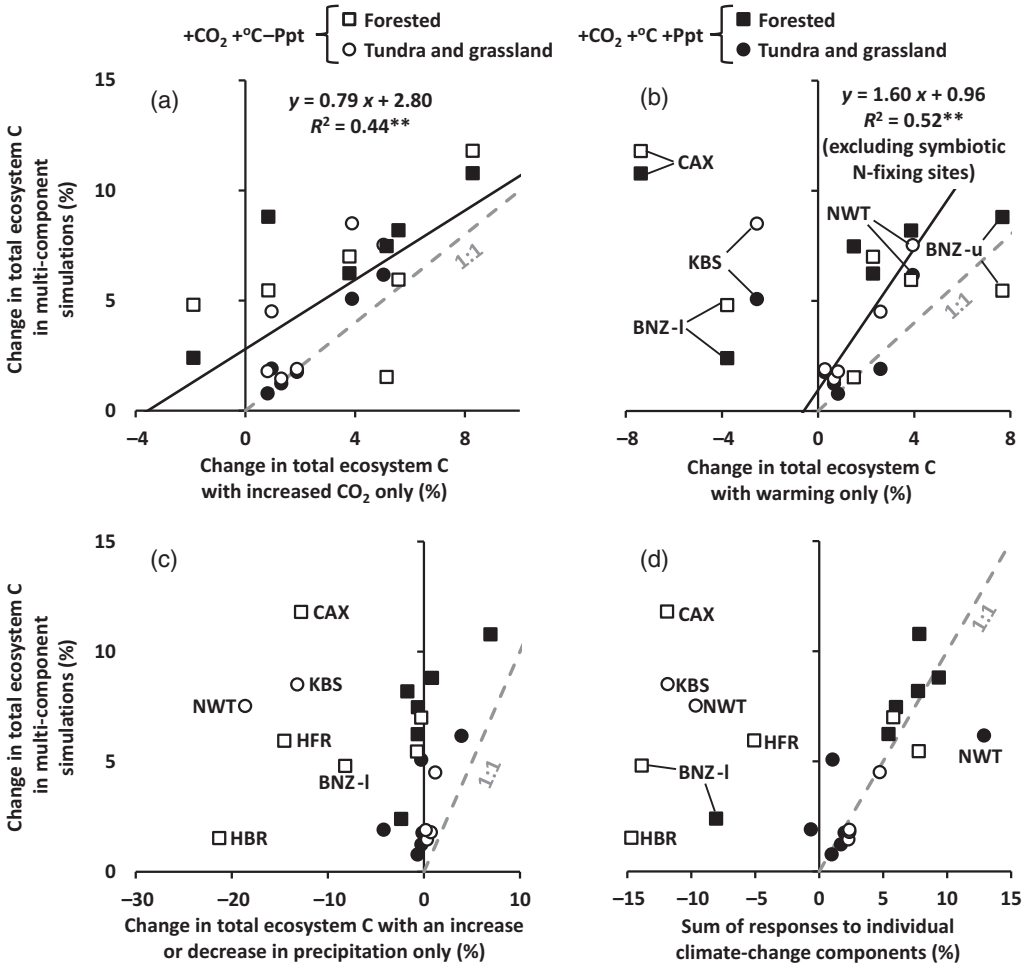

FIGURE 8 Change in total ecosystem C plotted against the responses to the individual climate-change components: (a) increased CO_2, (b) warming, (c) changes in precipitation, and (d) the sum of responses to the individual climate-change components. Squares are for the forested ecosystems (BNZ-l, BNZ-u, HBR, HFR, AND, and CAX). Circles are for tundra and grassland ecosystems (ARC-t, ARC-w, ARC-s, NWT, KBS, and KNZ). Ecosystems are identified in Table 1. The combined-component climate simulations with decreased precipitation are in open symbols and the combined-component climate simulations with increased precipitation are in filled symbols. **Regression $p < 0.01$.

for all but two of the ecosystems (near the 1:1 line in Figure 8d). That is, the response in the multi-component simulation is about equal to the sum of the responses in the single-component simulations. For the lowland boreal forest (BNZ-l) the interaction is synergistic because elevated CO_2 and warming stimulate plant production and redistribute N and P from soil to vegetation enough to compensate for leaching losses of N and P (Figures 4 and 5). For the alpine dry meadow (NWT) the interaction is antagonistic because all three of the individual climate components increase N fixation and P retention but constraints on these processes limit the magnitudes in the multi-component simulations to less than the sum of the responses to the individual components (Figures 4 and 5).

To help assess the relative importance of the N and P attribution factors in the multi-component climate-change simulations, we calculate type-II regressions (Sokal & Rohlf, 1995) across all 12 ecosystems of percent change in total ecosystem C versus the percent contribution by each attribution factor (red [N] and blue [P] lines in Figures 9 and 10). Analyzed across all ecosystems, the regressions for the redistribution of N and P from soil to vegetation have a slope near 1, indicating that this redistribution is the dominant factor contributing to C gain. The slopes for the other attribution factors are much steeper, indicating their weaker contribution to C gain when analyzed across all 12 ecosystems.

The importance of this N and P redistribution depends in part on the element concentrations in vegetation versus soil. A high C:N in vegetation relative to soil results in a large increase in total C when N is redistributed from soil to vegetation. Thus, the percent increase in ecosystem C is positively correlated with the ratio of vegetation C:N to soil C:N (ratio of ratios) for the multi-component simulations with both decreased

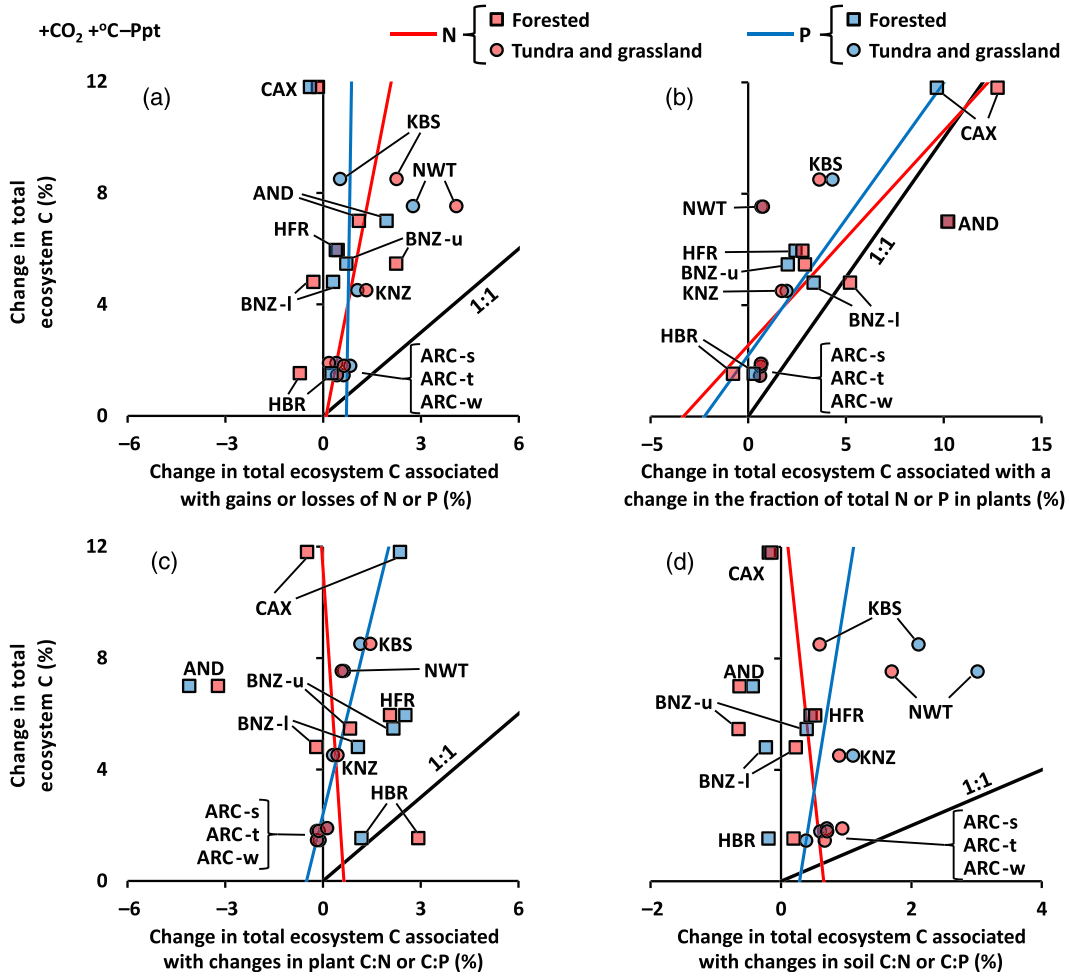

FIGURE 9 Changes in total ecosystem C in the combined climate-change simulations with decreased precipitation in relation to the change in total ecosystem C attributed to each of the N and P attribution factors (Equations 1–5). Results for the N-attribution factors are in red symbols and results for the P-attribution factors are in blue. Squares are for the forested ecosystems (BNZ-l, BNZ-u, HBR, HFR, AND, and CAX). Circles are for tundra and grassland ecosystems (ARC-t, ARC-w, ARC-s, NWT, KBS, and KNZ). Ecosystems are identified in Table 1. Red lines are type-II regressions through the N-attribution data and blue lines are type-II regressions through the P-attribution data. Black 1:1 lines are to help gauge the relative importance of each attribution factor; regression lines closer to the 1:1 line contribute more to the overall response.

($R = 0.64$, $p < 0.05$) and increased ($R = 0.66$, $p < 0.05$) precipitation. Similarly, the percent increase in ecosystem C is positively correlated with the ratio of vegetation to soil C:P for the multi-component simulations with decreased ($R = 0.75$, $p < 0.01$) and increased ($R = 0.65$, $p < 0.05$) precipitation. The relatively high C:N and C:P of trees causes forested ecosystems to have a higher percent increase in ecosystem C than the tundra and grassland ecosystems, especially in the simulations where precipitation increased (Figures 9 and 10). The only non-forested ecosystems with high percent C gains are the alpine dry meadow (NWT) and the restored prairie (KBS), both of which have symbiotic N fixation.

In all five ecosystems that have symbiotic N fixation (sites with leguminous and/or actinorhizal species), the rate of N fixation increases in the multi-component simulations, except in the tropical rainforest (CAX) when precipitation decreases. Despite the general increase in fixation, leaching losses result in both the boreal forests (BNZ-l and BNZ-u) losing N in the multi-component simulations with increased precipitation. In the same simulations, the lowland boreal forest (BNZ-l) also loses a small amount of P while in the upland boreal forest (BNZ-u), higher P demand and consequent higher retention efficiency results in a small P gain (Figures 5 and 10). With decreased precipitation in the multi-component simulations, water limitation in the lowland boreal forest decreases nutrient demand resulting in a small loss of N. Because of symbiotic N fixation in the alpine dry meadow (NWT) and the restored prairie (KBS), the C gain associated with increased ecosystem N is larger than the C gain associated with increased ecosystem P in the multi-

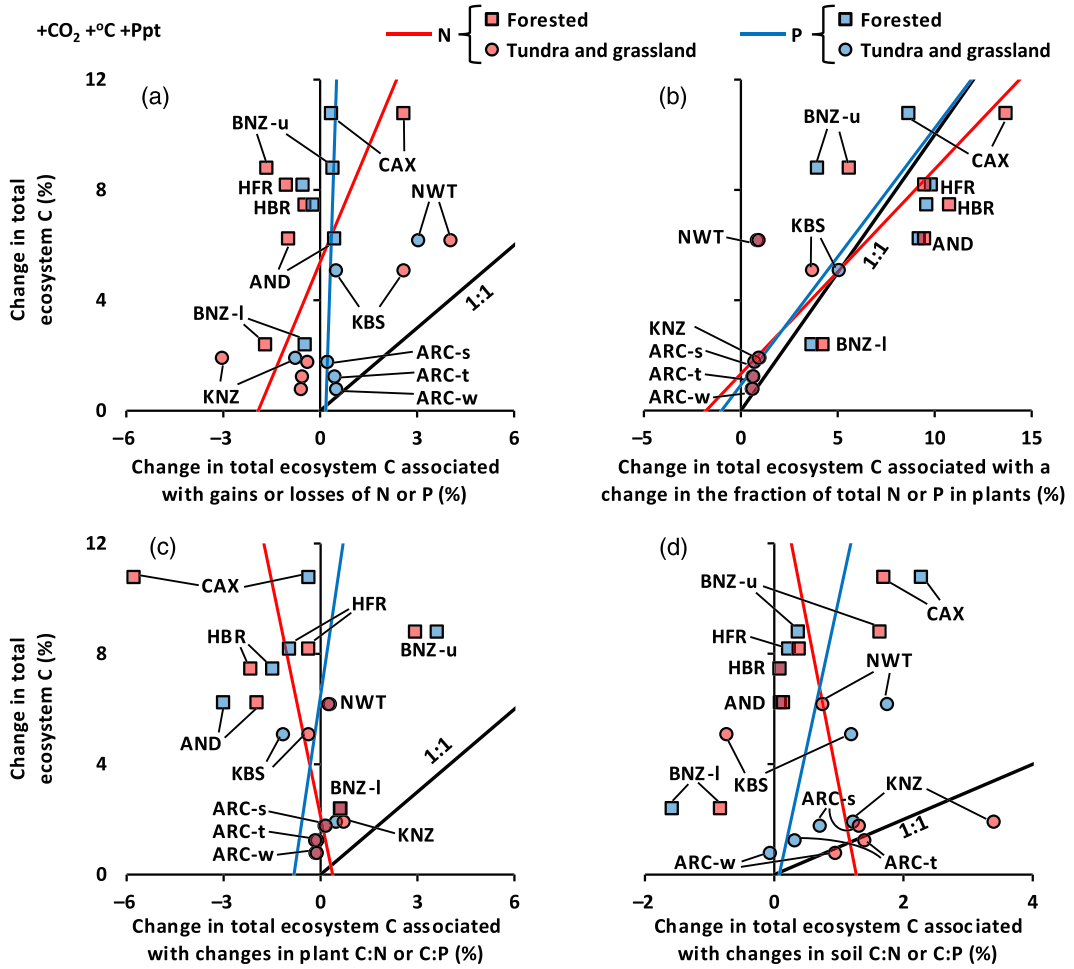

FIGURE 10 Changes in total ecosystem C in the combined climate-change simulations with increased precipitation in relation to the change in total ecosystem C attributed to each of the N and P attribution factors (Equations 1–5). Results for the N-attribution factors are in red symbols and results for the P-attribution factors are in blue. Squares are for the forested ecosystems (BNZ-l, BNZ-u, HBR, HFR, AND, and CAX). Circles are for tundra and grassland ecosystems (ARC-t, ARC-w, ARC-s, NWT, KBS, and KNZ). Ecosystems are identified in Table 1. Red lines are type-II regressions through the N-attribution data and blue lines are type-II regressions through the P-attribution data. Black 1:1 lines are to help gauge the relative importance of each attribution factor; regression lines closer to the 1:1 line contribute more to the overall response.

component climate simulations with both decreased (Figure 9a) and increased (Figure 10a) precipitation. Similarly, both ecosystems increase soil C:P more than soil C:N (Figures 8d and 9d) because of this difference in N versus P gain. In contrast, the tropical rainforest (CAX) accumulates neither N nor P in the multi-component simulation with decreased precipitation and the soil C:N and C:P remain almost constant (Figures 8a,d). More N than P is redistributed from soil to vegetation (Figure 9b), which is compensated by an increase in the vegetation C:P and a small decrease in the vegetation C:N (Figure 9c). In the multi-component simulation with increased precipitation, the tropical rainforest accumulates N through symbiotic N fixation (Figure 10a) and compensates with a larger increase in the soil C:P than C:N and a large decrease in the vegetation C:N (Figure 10c).

Despite a four- to five-fold difference in the ratio of plant to soil C, N, and P, the three arctic ecosystems cluster tightly with respect to the percent change in ecosystem C and the fraction of that change attributable to each of the attribution factors (Figures 9 and 10). In the combined-component simulations with decreased precipitation, all three ecosystems accumulate a small amount of N and P because of the decrease in leaching losses, redistribute a small amount of N and P from soil to vegetation, and increase the C:N and C:P of soil (Figure 9). In the combined-component simulation with increased precipitation, these three arctic ecosystems lose N through increased leaching but retain and accumulate a small amount of P (Figure 10a). This higher retention of P over N indicates a tendency toward P limitation in these simulations, which is consistent with the findings of Yang

et al. (2021) for the response of tundra during permafrost thaw. Nevertheless, this difference in N versus P retention is compensated by a larger increase in the soil C:N than C:P ratio (Figure 10d). The tallgrass prairie (KNZ) responds similarly to the arctic sites, but with a stronger redistribution of N and P from soil to vegetation and a larger increase in soil C:N and C:P, and consequently, a larger percent increase in total ecosystem C (Figures 9 and 10).

Interactions between N and P: Within treatments across attribution factors

We analyze the interactions between N- and P-attribution factors by first calculating correlations within treatments across attribution factors (Table 3). We then regress these correlations against various ecosystem characteristics or combinations of characteristics (Table 1). Here we present only the most noteworthy relationships (Tables 3 and 4). Because correlations are asymptotic to both −1 and 1, we linearize the correlation data using a modified arcsine transform before performing the regressions:

$$y = \sin^{-1}\left(\sqrt{0.5\,(1+R)}\right) \tag{7}$$

where R is the correlation coefficient between N- and P-attribution factors and y is the transformed value.

Within treatments across attribution factors the correlations varied widely among ecosystems (Table 3). The degree of correlation between N- and P-attribution factors is not significantly related to the percent change in vegetation, soil, or total C except for the multi-component simulation with increased precipitation ($p \sim 0.05$). The correlation between N and P attribution factors for each treatment decreases as the fraction of plant N uptake in the form of DON and symbiotic N fixation increases (see regression at bottom of Table 3). The decline in correlation is strongest for elevated CO_2 alone, warming alone, and increasing precipitation alone. Unlike uptake of NH_4 and NO_3, which roughly parallel the uptake of PO_4, there is no source of P in the model that is parallel either to DON uptake directly from soil organic matter or to symbiotic N fixation. However, there are P parallels to DON uptake and symbiotic N fixation in nature. For example, mycorrhizal acquisition of organic P (Bunn et al., 2019) parallels DON uptake and

TABLE 4 Correlation between N- versus P-attribution factors for each ecosystem within attribution factors across treatments.

	Correlation between N-attribution factors and P-attribution factors				
Site	Change in total ecosystem N versus P	Redistribution of N versus P between soil and vegetation	Change in vegetation C:N versus C:P	Change in soil C:N versus C:P	Interactions among N versus P attribution factors
ARC-t	0.45	1.00**	0.99**	0.77	0.91*
ARC-w	0.52	1.00**	0.99**	0.34	0.97**
ARC-s	0.48	0.99**	1.00**	0.96**	0.96**
NWT	0.99**	1.00**	1.00**	0.98**	1.00**
KBS	0.93**	0.98**	0.88*	0.79	0.90*
KNZ	0.94**	1.00**	0.98**	0.76	0.80
BNZ-l	0.59	0.98**	0.77	0.84*	0.73
BNZ-u	0.71	0.93**	0.90*	0.29	0.94**
HBR	0.76	1.00**	0.57	0.97**	0.30
HFR	0.99**	1.00**	0.91*	0.99**	0.75
AND	0.78	1.00**	0.99**	1.00**	1.00**
CAX	0.90*	0.99**	0.91*	0.98**	0.28
Regression	$y = 1.72x + 1.12$	$y = 1.75z + 1.49$	$y = 4.44z + 1.31$	$y = -2.16w + 3.34$	$y = 7.21z + 1.15$
R^2	0.48	0.28	0.33	0.36	0.41
p	0.011	0.075	0.052	0.039	0.024

Note: *$p < 0.05$, df = 4, **$p < 0.01$, df = 4. Regressions relate the correlations for each attribution factor, across sites, to either the openness of N cycle (x), the openness of P cycle (z), or the fraction of ecosystem N in soil (w). To linearize correlations for the regression, they are transformed with a modified arcsine transform (Equation 7). Sites are identified in Table 1.

mycorrhizal weathering of apatite (Blum et al., 2002) parallels symbiotic N fixation in ecosystems where apatite is present in the rooting/mycorrhizal zone (unlikely at CAX; Porder & Hilley, 2011). These are processes that could be added to the model, but the data needed to calibrate these processes are not yet available.

Thus, the N and P characteristics of an ecosystem do not necessarily change in parallel in its response to a particular treatment. The degree to which N and P attribution factors of the ecosystem change in parallel does not constrain ecosystem C gains and losses in our simulations, indicating some independence between N and P constraints and some degree of desynchronization of the two cycles in response to climate change. This desynchronization is facilitated in our model by the diversity of N sources to vegetation for which there are no analogous P sources.

Interactions between N and P: Within attribution factors across treatments

The correlations between N- and P-attribution factors across treatments are generally strong (Table 4). The highest correlations are for the net redistribution of N and P between soil and vegetation and for changes in the C:N and C:P of vegetation, indicating the tight coupling of the N and P cycle and tight regulation of vegetation stoichiometry in our model. Both correlations increase weakly with the openness of the P cycle ($p \sim 0.075$ and $p \sim 0.052$, respectively). However, these relationships to the P-cycle openness have little ecological meaning because all the correlations are high; thus, the redistributions of N and P are tightly parallel and the C:N:P stoichiometry of vegetation is tightly regulated in our model.

The correlations between net gain or losses of N versus P range from 0.45 to 0.99 and increase with the openness of the N cycle (Table 4; $p \sim 0.011$), but not with the openness of the P cycle. Thus, ecosystems with open N cycles can adjust N gains and losses to match the net gains in P. In the model, it is more difficult for ecosystems with less open N cycles to make this adjustment, at least within the 100 years of the simulations. In our simulations, the N cycle is more open than the P cycle in all but three of the ecosystems (Table 1); because of its openness, the N cycle adjusts to the P cycle and not the other way around.

The correlations between changes in soil C:N and C:P ratios range from 0.34 to 1. The correlations decrease as the fraction of total ecosystem C, N, or P that is in soil increases (Table 4, strongest relation for N: $p \sim 0.039$). Rather than buffering the soil stoichiometry, a large soil stock opens more opportunities for N and P to change independently. Because most of the total-soil N and P are in dead organic matter rather than microbial biomass, the soil C:N:P is not as strongly constrained by microbial stoichiometry as the vegetation C:N:P is by plant stoichiometry.

The correlations between the N and P interactive terms in the attribution analysis increase with the openness of the P cycle (Table 4; $p \sim 0.024$), but not with the openness of the N cycle. Because this term represents all potential interactions among four primary attribution factors, it is difficult to attribute ecological meaning to its relation to the openness of the P cycle. Nevertheless, the results relating correlations between net gain or losses of N versus P to the openness of the N cycle but not the P cycle (above) indicate that the N cycle adjusts to the P cycle. The relation of the interactive terms to the openness of the P cycle might simply reflect the constraints imposed by the P cycle and a more open P cycle opens more opportunities for the four attribution factors to interact.

Thus, the ecosystem characteristics that influence the correlation between N and P differ for each of the attribution factors. This difference in the ecosystem characteristics influencing each attribution factor explains why the within-treatment, across-attribution factor correlations are generally weaker than the within-attribution factor, across-treatment correlations.

Implications, cautions, and caveats

Thornton et al. (2009) demonstrated the importance of including N feedbacks in assessing responses of the terrestrial biosphere to elevated CO_2 and climate change. Our analyses indicate that P also plays an important role. Co-limitation of ecosystems by N and P is widely recognized (Davidson & Howarth, 2007; Du et al., 2020; Elser et al., 2007; Klodd et al., 2016; Ostertag & DiManno, 2016), and the relation of this co-limitation to soil parent material and climate is becoming clear (Augusto et al., 2017). With this recognition, both N and P are increasingly being incorporated into global models (Goll et al., 2012; Thum et al., 2019; Wang et al., 2010; Yang et al., 2019). We build on this general understanding by showing how global change alters the synchronization between N and P cycles and how these responses differ among ecosystems. Desynchronization of N and P cycles is a likely response to many types of disturbance including climate change; recovery from that disturbance involves reestablishing that synchronization (Rastetter et al., 2013). The divergence in N versus P attribution among ecosystems is especially large under elevated CO_2 and in simulations where plant N acquisition relies on N

fixation or organic N uptake. These results highlight the importance of the ongoing uncertainty in how plant nutrient acquisition influences C storage under global change. For example, mycorrhizal acquisition of P from SOM or apatite parallel DON use by plants and symbiotic N fixation, which could help maintain synchrony in our model between N and P cycles in response to climate change and result in stronger C sequestration in those ecosystems constrained by P limitation.

Compiling the data needed to do this type of analysis is difficult. We fill data gaps as best we can but are still left with questions. For example, processes that are clearly important at some sites are not reported for others. Does the process not occur at these sites, or has it just not been investigated (e.g., N fixation, DON leaching loss and DON use by vegetation)? Details about the P cycle are particularly problematic (e.g., gross mineralization and immobilization, plant access to organic forms of P). The lack of stable-isotope tracers makes it difficult to quantify the P pools and fluxes necessary to inform a more complete model, although some progress on methods is being made (see Helfenstein et al., 2018). In addition, sampling standards reflect the specific goals of the original study and do not necessarily apply to questions about whole-ecosystem nutrient cycling. Sampling protocols and methods also differ among ecosystem types; methods developed for forests might not apply, or be applied, in grasslands or tundra. These differences can introduce biases when doing cross-biome analyses. For example, exchangeable P methods have been developed for soils of different pH and comparing them across natural ecosystems can be problematic. Such limitations are the major impetus for our heuristic rather than predictive goal.

The same difficulty in compiling data to calibrate the model also limits the ability to constrain sensitivity analyses on the simulations. A proper constraint of such an analysis would require quantification of the variability of each of the variables in the analysis. Otherwise, the analysis would need to rely on an arbitrary variance (e.g., ±10%), which can lead to misleading conclusions because it amplifies the significance of variables with lower actual variance and underestimates the significance of variables with higher actual variance. Nevertheless, a comparison of the responses to CO_2 and climate among the ecosystems in our analysis does provide some assessment of sensitivity. For example, the three arctic tundra ecosystems tend to cluster together in most of our analyses despite an approximately three-fold difference in vegetation biomass and an approximately two-fold difference in SOM (e.g., Table 2, Figures 9 and 10). Similarly, the northern hardwood and transition oak–maple forests tend to cluster in our analyses (Figure 10) except when precipitation is decreased (Figure 9). In contrast, although having similar characteristics, the restored and native tallgrass prairies diverge widely in our analyses (Table 2, Figures 9 and 10). The results discussed above explain most of this pattern in terms of the mechanisms represented in our model. Thus, better quantification of the stocks and fluxes of elements in ecosystems as well as the variance in these stocks and fluxes is needed to improve predictions of ecosystem response to changes in CO_2 and climate.

There are also clear limitations with the MEL model itself. The cost of making the model broadly applicable across a diverse set of ecosystems is that details specific to particular ecosystems can be oversimplified. These details include the representation of the biophysical controls on temperature and moisture in permafrost versus temperate or tropical soils, the complexity of microbial responses to temperature and moisture in different soils, and the effects of species interactions in different types of plant communities. The P cycle in the model is the least well-developed component. For example, C gain in some of our simulations is possible because of N accumulation in the ecosystem through symbiotic or non-symbiotic N fixation, but there is no analogue for P accumulation in the model. Could mycorrhizal weathering of primary P minerals provide that analogue to symbiotic N fixation (Blum et al., 2002)? Are N-fixation and mineral P weathering directly coupled (Perakis & Pett-Ridge, 2019)? Biotic facilitation of P (and N) acquisition from SOM is also important (Bunn et al., 2019) but missing from the current model. Similarly, the effects and costs of both plant and microbial exo-enzymes (Margalef et al., 2017) are not explicitly represented in the model. Despite having flexible vegetation and soil stoichiometry, the vegetation pools simulated by MEL tend to adhere closely to their parameterized targets, a result that could be better evaluated with observations from long-term ecosystem studies. Collectively, these deficiencies contribute to the imbalance between the representation of N and P in the MEL model and should be addressed for future analyses.

CONCLUSIONS

Our analyses indicate that elevated CO_2 and warming should typically result in ecosystem C gain. Most of this C gain is a result of elevated CO_2. However, warmer temperatures should accelerate nutrient cycling, enhance fertility, and stimulate production and thereby result in a net transfer of nutrients from soil to vegetation and an associated C gain by the ecosystem. Enhanced N availability might also inhibit symbiotic N fixation, which

could reduce C gains in some ecosystems. The effects of changes in precipitation are less clear in our simulations. Decreased precipitation alone has a substantial effect in ecosystems where the soil cannot hold enough water to supply the vegetation through the drought period. However, increased water-use efficiency with elevated CO_2 and increased fertility with warming compensate for the drought effects in our simulations. Higher intensities of precipitation could enhance leaching and erosional losses of N and P, which could reduce future C gain in some ecosystems, especially if the high intensity precipitation corresponds with periods when plants are less active and nutrients have built up in soil solution. Conversely, decreased precipitation intensity could enhance N and P retention, allowing enhanced future C gain if the magnitude and timing of the decrease in precipitation does not impose water limitation.

As indicated above, N and P availability will constrain future C gain, but these constraints will vary among ecosystems based on the ability of the ecosystem to accumulate N and P, to redistribute N and P from soil to vegetation, and to change the stoichiometry of vegetation and soils. Our analyses indicate that in forest ecosystems, which have high C:N and C:P ratios in vegetation, a redistribution of N and P from soil (lower C:N and C:P) to vegetation will account for most of this C gain. In contrast, in tundra and grassland ecosystems, which tend to have high turnover rates of vegetation biomass, an increase in soil C:N and C:P ratios could also account for a large part of the C gain in response to future climate change. In addition, controls on gains and losses of N and P from ecosystems vary but need to be assessed to evaluate the potential for C sequestration.

Changes in the relation of C to N in response to changes in CO_2 and climate do not necessarily parallel the analogous changes in the relation of C to P. For example, a gain in ecosystem C might be associated with an accumulation of ecosystem N without an accompanying accumulation of P if the C:P ratios of ecosystem components increase. Similarly, a gain in C resulting from a net transfer on N from soil to vegetation might be accommodated by an increase in vegetation C:P ratio and an increase in soil C:N ratio. Our analysis indicates that the mechanisms by which C is sequestered relative to N versus P are not inextricably linked to one another and thus vary among ecosystems. The divergence between N versus P mechanisms of C sequestration is particularly large for ecosystems with more open N cycle resulting, for example, from N fixation. Because N cycles are generally more open than P cycles, ecosystems can adjust N gains and losses to match the net gains in P. Thus, our results indicate that the N cycle more readily adjusts to changes in the P cycle than the other way around.

ACKNOWLEDGMENTS

This material is based on work supported by the National Science Foundation under Grant No. 1651722 as well through the NSF LTER Program 1637459, 2220863 (ARC), 1637686 (NWT), 1832042 (KBS), 2025849 (KNZ), 1636476 (BNZ), 1637685 (HBR), 1832210 (HFR), 2025755 (AND). We also acknowledge NSF grants 1637653 and 1754126 (INCyTE RCN), and DOE grant DESC0019037. We also acknowledge support through the USDA Forest Service Hubbard Brook Experimental Forest, North Woodstock, New Hampshie (USDA NIFA 2019-67019-29464) and Pacific Northwest Research Station, Corvallis, Oregon. Opinions are those of the authors and do not reflect those of the National Science Foundation or the USDA Forest Service. Any use of trade, firm, or product names is for descriptive purposes only and does not imply endorsement by the U.S. Government. Some data were provided by the Climate and Hydrology Database Projects (Henshaw et al., 2021). We would also like to thank Eve-Lyn Hinckley, Chris Johnson, and Timothy Seastedt for assistance compiling the data sets used in this analysis. We respectfully acknowledge the Indigenous Peoples on whose ancestral lands this research was conducted: the Nunamiut, Gwich'in, Koyokuk, and Iñupiaq peoples of Northern Alaska (ARC), the Ute, Arapaho, and Cheyenne peoples of Colorado (NWT), the Potawatomi, Odawa, and Ojibwe peoples of South-Central Michigan (KBS), the Kansa and Potawatomie peoples of Kansas (KNZ), the lower Tanana Dene people of interior Alaska (BNZ), the Pennacook and Abenaki people of New Hampshire (HBR), the Nipmuc people of Central Massachusetts (HFR), the Kalapuya and Molalla peoples of Western Oregon (AND), the Tupi and Tupi-Guarani peoples of the Brazilian Amazon (CAX), and the Paleo-American peoples of the Americas.

CONFLICT OF INTEREST

The authors have no conflicts of interest.

DATA AVAILABILITY STATEMENT

Code (bkwiatkowski, 2022) is available on Zenodo at https://doi.org/10.5281/zenodo.6502583. Data used in the simulations (Rastetter et al., 2022a, 2022b) are available from the Environmental Data Initiative at https://doi.org/10.6073/pasta/b737b5f0855aa7afeda68764e77aec2a and https://doi.org/10.6073/pasta/7ca56dfbe6c9bedf5126e9ff7e66f28d.

ORCID

Edward B. Rastetter https://orcid.org/0000-0002-8620-5431

Bonnie L. Kwiatkowski https://orcid.org/0000-0003-0158-9753

David W. Kicklighter https://orcid.org/0000-0001-6820-2651
Audrey Barker Plotkin
Helene Genet https://orcid.org/0000-0003-4537-9563
Jesse B. Nippert https://orcid.org/0000-0002-7939-342X
Kimberly O'Keefe https://orcid.org/0000-0001-7799-0514
Steven S. Perakis https://orcid.org/0000-0003-0703-9314
Stephen Porder https://orcid.org/0000-0002-5279-766X
Sarah S. Roley https://orcid.org/0000-0002-6733-9338
Roger W. Ruess https://orcid.org/0000-0003-4557-6161
Jonathan R. Thompson https://orcid.org/0000-0003-0512-1226
William R. Wieder https://orcid.org/0000-0001-7116-1985
Kevin Wilcox https://orcid.org/0000-0001-6829-1148
Ruth D. Yanai https://orcid.org/0000-0001-6987-2489

REFERENCES

Arora, V. K., A. Katavouta, R. G. Williams, C. D. Jones, V. Brovkin, P. Friedlingstein, J. Schwinger, et al. 2020. "Carbon–Concentration and Carbon–Climate Feedbacks in CMIP6 Models and their Comparison to CMIP5 Models." *Biogeosciences* 17(16): 4173–222. https://doi.org/10.5194/bg-17-4173-2020.

Augusto, L., D. L. Achat, M. Jonard, D. Vidal, and B. Ringeval. 2017. "Soil Parent Material—A Major Driver of Plant Nutrient Limitations in Terrestrial Ecosystems." *Global Change Biology* 23(9): 3808–24. https://doi.org/10.1111/gcb.13691.

Austin, A. T., and P. M. Vitousek. 2012. "Introduction to a Virtual Special Issue on Ecological Stoichiometry and Global Change." *New Phytologist* 196(3): 649–51. https://doi.org/10.1029/2019GB006393.

Barford, C. C., S. C. Wofsy, M. L. Goulden, J. W. Munger, E. H. Pyle, S. P. Urbanski, L. Hutyra, S. R. Saleska, D. Fitzjarrald, and K. Moore. 2001. "Factors Controlling Long-and Short-Term Sequestration of Atmospheric CO2 in a Mid-Latitude Forest." *Science* 294((5547): 1688–91. https://doi.org/10.1126/science.1062962.

Bastos, A., M. O'Sullivan, P. Ciais, D. Makowski, S. Sitch, P. Friedlingstein, F. Chevallier, et al. 2020. "Sources of Uncertainty in Regional and Global Terrestrial CO2 Exchange Estimates." *Global Biogeochemical Cycles* 34(2): e2019GB006393. https://doi.org/10.1029/2019GB006393.

bkwiatkowski. 2022. "bkwiatkowski/MELVI: MELVI v2.8.5 (v2.8.5)." Zenodo. https://doi.org/10.5281/zenodo.6502583.

Blum, J. D., A. Klaue, C. A. Nezat, C. T. Driscoll, C. E. Johnson, T. G. Siccama, C. Eagar, T. J. Fahey, and G. E. Likens. 2002. "Mycorrhizal Weathering of Apatite as an Important Calcium Source in Base-Poor Forest Ecosystems." *Nature* 417(6890): 729–31. https://doi.org/10.1038/nature00793.

Boyle, J. F., R. C. Chiverrell, S. A. Norton, and A. J. Plater. 2013. "A Leaky Model of Long-Term Soil Phosphorus Dynamics." *Global Biogeochemical Cycles* 27(2): 516–25. https://doi.org/10.1002/gbc.20054.

Bret-Harte, M., E. Euskirchen, K. Griffin, and G. Shaver. 2019. "Eddy Flux Measurements, Tussock Station, Imnavait Creek, Alaska - 2018 - Provisional ver 1." Environmental Data Initiative. https://doi.org/10.6073/pasta/5cc4d550ef863e80e781db290b6ae6ba.

Bunn, R. A., D. T. Simpson, L. S. Bullington, Y. Lekberg, and D. P. Janos. 2019. "Revisiting the 'Direct Mineral cycling' hypothesis: Arbuscular Mycorrhizal Fungi Colonize Leaf Litter, but Why?" *The ISME Journal* 13(8): 1891–8. https://doi.org/10.1038/s41396-019-0403-2.

Campbell, J. L., L. E. Rustad, E. W. Boyer, S. F. Christopher, C. T. Driscoll, I. J. Fernandez, P. M. Groffman, et al. 2009. "Consequences of Climate Change for Biogeochemical Cycling in Forests of Northeastern North America." *Canadian Journal of Forest Research* 39(2): 264–84. https://doi.org/10.1139/X08-104.

Chapin, F. S. I. I. I., G. M. Woodwell, J. T. Randerson, E. B. Rastetter, G. M. Lovett, D. D. Baldocchi, D. A. Clark, et al. 2006. "Reconciling Carbon-Cycle Concepts, Terminology, and Methods." *Ecosystems* 9(7): 1041–50. https://doi.org/10.1007/s10021-005-0105-7.

Davidson, E. A., and R. W. Howarth. 2007. "Nutrients in Synergy." *Nature* 449(7165): 1000–1. https://doi.org/10.1038/4491000a.

Du, E., C. Terrer, A. F. A. Pellegrini, A. Ahlström, C. J. van Lissa, X. Zhao, N. Xia, X. Wu, and R. B. Jackson. 2020. "Global Patterns of Terrestrial Nitrogen and Phosphorus Limitation." *Nature Geoscience* 13(3): 221–6. https://doi.org/10.1038/s41561-019-0530-4.

Eby, M., A. J. Weaver, K. Alexander, K. Zickfeld, A. Abe-Ouchi, A. A. Cimatoribus, E. Crespin, et al. 2013. "Historical and Idealized Climate Model Experiments: An Intercomparison of Earth System Models of Intermediate Complexity." *Climate of the Past* 9(3): 1111–40. https://doi.org/10.5194/cp-9-1111-2013.

Elser, J. J., M. E. S. Bracken, E. E. Cleland, D. S. Gruner, W. S. Harpole, H. Hillebrand, J. T. Ngai, E. W. Seabloom, J. B. Shurin, and J. E. Smith. 2007. "Global Analysis of Nitrogen and Phosphorus Limitation of Primary Producers in Freshwater, Marine and Terrestrial Ecosystems." *Ecology Letters* 10(12): 1135–42. https://doi.org/10.1111/j.1461-0248.2007.01113.x.

Euskirchen, E. S., C. W. Edgar, M. R. Turetsky, M. P. Waldrop, and J. W. Harden. 2014. "Differential Response of Carbon Fluxes to Climate in Three Peatland Ecosystems that Vary in the Presence and Stability of Permafrost." *Journal of Geophysical Research: Biogeosciences* 119(8): 1576–95. https://doi.org/10.1002/2014JG002683.

Finzi, A. C., M.-A. Giasson, A. A. Barker Plotkin, J. D. Aber, E. R. Boose, E. A. Davidson, M. C. Dietze, et al. 2020. "Carbon Budget of the Harvard Forest Long-Term Ecological Research Site: Pattern, Process, and Response to Global Change." *Ecological Monographs* 90(4): e01423. https://doi.org/10.1002/ecm.1423.

Gerten, D., Y. Luo, G. Le Maire, W. J. Parton, C. Keough, E. Weng, C. Beier, et al. 2008. "Modelled Effects of Precipitation on Ecosystem Carbon and Water Dynamics in Different Climatic Zones." *Global Change Biology* 14(10): 2365–79. https://doi.org/10.1111/j.1365-2486.2008.01651.x.

Goll, D. S., V. Brovkin, B. R. Parida, C. H. Reick, J. Kattge, P. B. Reich, P. M. Van Bodegom, and Ü. Niinemets. 2012. "Nutrient Limitation Reduces Land Carbon Uptake in Simulations with a Model of Combined Carbon, Nitrogen and Phosphorus Cycling." *Biogeosciences* 9(9): 3547–69. https://doi.org/10.5194/bg-9-3547-2012.

Gress, S. E., T. D. Nichols, C. C. Northcraft, and W. T. Peterjohn. 2007. "Nutrient Limitation in Soils Exhibiting Differing

Nitrogen Availabilities: What Lies beyond Nitrogen Saturation?" *Ecology* 88(1): 119–30. https://doi.org/10.1890/0012-9658(2007)88%5B119:NLISED%5D2.0.CO;2.

Helfenstein, J., F. Tamburini, C. von Sperber, M. S. Massey, C. Pistocchi, O. A. Chadwick, P. M. Vitousek, R. Kretzschmar, and E. Frossard. 2018. "Combining Spectroscopic and Isotopic Techniques Gives a Dynamic View of Phosphorus Cycling in Soil." *Nature Communications* 9(1): 1–9. https://doi.org/10.1038/s41467-018-05731-2.

Henshaw, D. Z., S. Z. Remillard, Y. Xia, J. Brunt, and W. Sheldon. 2021. "ClimHyrdoDB Archive: Meteorologic and Hydrologic Observations from LTER and USFS Sites, 2001–2020 - Orignal Database Format ver 4." Environmental Data Initiative. https://doi.org/10.6073/pasta/b9c3b821f3b7b2fba9bcc85fbb015773.

Herrick, J. D., and R. B. Thomas. 2001. "No Photosynthetic Down-Regulation in Sweetgum Trees (*Liquidambar styraciflua* L.) after Three Years of CO2 Enrichment at the Duke Forest FACE Experiment." *Plant, Cell & Environment* 24(1): 53–64. https://doi.org/10.1046/j.1365-3040.2001.00652.x.

Iverson, L. R., F. R. Thompson, S. Matthews, M. Peters, A. Prasad, W. D. Dijak, J. Fraser, et al. 2017. "Multi-Model Comparison on the Effects of Climate Change on Tree Species in the Eastern US: Results from an Enhanced Niche Model and Process-Based Ecosystem and Landscape Models." *Landscape Ecology* 32(7): 1327–46. https://doi.org/10.1007/s10980-016-0404-8.

Jiang, Y., E. B. Rastetter, A. V. Rocha, A. R. Pearce, B. L. Kwiatkowski, and G. R. Shaver. 2015. "Modeling Carbon–Nutrient Interactions during the Early Recovery of Tundra after Fire." *Ecological Applications* 25: 1640–52. https://doi.org/10.1890/14-1921.1.

Klodd, A. E., J. B. Nippert, Z. Ratajczak, H. Waring, and G. K. Phoenix. 2016. "Tight Coupling of Leaf Area Index to Canopy Nitrogen and Phosphorus across Heterogeneous Tallgrass Prairie Communities." *Oecologia* 182(3): 889–98. https://doi.org/10.1007/s00442-016-3713-3.

Lawrence, D. M., R. A. Fisher, C. D. Koven, K. W. Oleson, S. C. Swenson, G. Bonan, N. Collier, et al. 2019. "The Community Land Model Version 5: Description of New Features, Benchmarking, and Impact of Forcing Uncertainty." *Journal of Advances in Modeling Earth Systems* 11(12): 4245–87. https://doi.org/10.1029/2018ms001583.

Leakey, A. D. B., K. A. Bishop, and E. A. Ainsworth. 2012. "A Multi-Biome Gap in Understanding of Crop and Ecosystem Responses to Elevated CO2." *Current Opinion in Plant Biology* 15(3): 228–36. https://doi.org/10.1016/j.pbi.2012.01.009.

Luo, Y., D. Gerten, G. Le Maire, W. J. Parton, E. Weng, X. Zhou, C. Keough, et al. 2008. "Modeled Interactive Effects of Precipitation, Temperature, and [CO2] on Ecosystem Carbon and Water Dynamics in Different Climatic Zones." *Global Change Biology* 14(9): 1986–99 10.1111/j.1365-2486.2008.01629.x.

Mack, M. C., E. A. G. Schuur, M. S. Bret-Harte, G. R. Shaver, and F. S. Chapin. 2004. "Ecosystem Carbon Storage in Arctic Tundra Reduced by Long-Term Nutrient Fertilization." *Nature* 431 (7007): 440–3. https://doi.org/10.1038/nature02887.

Margalef, O., J. Sardans, M. Fernández-Martínez, R. Molowny-Horas, I. A. Janssens, P. Ciais, D. Goll, et al. 2017. "Global Patterns of Phosphatase Activity in Natural Soils." *Scientific Reports* 7(1): 1–13. https://doi.org/10.1038/s41598-017-01418-8.

Martin-Benito, D., and N. Pederson. 2015. "Convergence in Drought Stress, but a Divergence of Climatic Drivers across a Latitudinal Gradient in a Temperate Broadleaf Forest." *Journal of Biogeography* 42(5): 925–37. https://doi.org/10.1111/jbi.12462.

McGuire, A. D., D. M. Lawrence, C. Koven, J. S. Clein, E. Burke, G. Chen, E. Jafarov, et al. 2018. "Dependence of the Evolution of Carbon Dynamics in the Northern Permafrost Region on the Trajectory of Climate Change." *Proceedings of the National Academy of Sciences USA* 115(15): 3882–7. https://doi.org/10.1073/pnas.1719903115.

Melillo, J. M., J. D. Aber, A. E. Linkins, A. Ricca, B. Fry, and K. J. Nadelhoffer. 1989. "Carbon and Nitrogen Dynamics along the Decay Continuum: Plant Litter to Soil Organic Matter." *Plant and Soil* 115(2): 189–98. https://doi.org/10.1007/BF02202587.

Melillo, J. M., J. M. Reilly, D. W. Kicklighter, A. C. Gurgel, T. W. Cronin, S. Paltsev, B. S. Felzer, X. Wang, A. P. Sokolov, and C. A. Schlosser. 2009. "Indirect Emissions from Biofuels: How Important?" *Science* 326(5958): 1397–9. https://doi.org/10.1126/science.1180251.

Monier, E., D. W. Kicklighter, A. P. Sokolov, Q. Zhuang, I. N. Sokolik, R. Lawford, M. Kappas, S. V. Paltsev, and P. Y. Groisman. 2017. "A Review of and Perspectives on Global Change Modeling for Northern Eurasia." *Environmental Research Letters* 12(8): 083001. https://doi.org/10.1088/1748-9326/aa7aae.

Monier, E., S. Paltsev, A. Sokolov, Y.-H. H. Chen, X. Gao, Q. Ejaz, E. Couzo, et al. 2018. "Toward a Consistent Modeling Framework to Assess Multi-Sectoral Climate Impacts." *Nature Communications* 9(1): 1–8. https://doi.org/10.1038/s41467-018-02984-9.

National Ecological Observatory Network (NEON). 2021. "Bundled Data Products—Eddy Covariance, RELEASE-2021 (DP4.00200.001)." https://doi.org/10.48443/bway-hc74. https://data.neonscience.org.

Ollivier, J., S. Töwe, A. Bannert, B. Hai, E.-M. Kastl, A. Meyer, M. X. Su, K. Kleineidam, and M. Schloter. 2011. "Nitrogen Turnover in Soil and Global Change." *FEMS Microbiology Ecology* 78(1): 3–16. https://doi.org/10.1111/j.1574-6941.2011.01165.x.

Oreskes, N., K. Shrader-Frechette, and K. Belitz. 1994. "Verification, Validation, and Confirmation of Numerical Models in the Earth Sciences." *Science* 263(5147): 641–6. https://doi.org/10.1126/science.263.5147.641.

Ostertag, R., and N. M. DiManno. 2016. "Detecting Terrestrial Nutrient Limitation: A Global Meta-Analysis of Foliar Nutrient Concentrations after Fertilization." *Frontiers in Earth Science* 4: 23. https://doi.org/10.3389/feart.2016.00023.

Paschalis, A., G. G. Katul, S. Fatichi, S. Palmroth, and D. Way. 2017. "On the Variability of the Ecosystem Response to Elevated Atmospheric CO2 across Spatial and Temporal Scales at the Duke Forest FACE Experiment." *Agricultural and Forest Meteorology* 232: 367–83. https://doi.org/10.1016/j.agrformet.2016.09.003.

Pearce, A. R., E. B. Rastetter, B. L. Kwiatkowski, W. B. Bowden, M. C. Mack, and Y. Jiang. 2015. "Recovery of Arctic Tundra from Thermal Erosion Disturbance Is Constrained by Nutrient Accumulation: A Modeling Analysis." *Ecological Applications* 25(5): 1271–89. https://doi.org/10.1890/14-1323.1.

Perakis, S. S., and J. C. Pett-Ridge. 2019. "Nitrogen-fixing red alder trees tap rock-derived nutrients." *Proceedings of the National Academy of Sciences USA* 116(11): 5009–14. https://doi.org/10.1073/pnas.1814782116.

Porder, S., and G. E. Hilley. 2011. "Linking Chronosequences with the Rest of the World: Predicting Soil Phosphorus Content in Denuding Landscapes." *Biogeochemistry* 102(1): 153–66. https://doi.org/10.1007/s10533-010-9428-3.

Press, W. H., B. P. Flannery, S. A. Teukolsky, and W. T. Vetterling. 1986. *Numerical Recipes: The Art of Scientific Computing*. Cambridge: Cambridge University Press.

Rastetter, E. B. 1996. "Validating Models of Ecosystem Response to Global Change." *Bioscience* 46(3): 190–8 https://www.jstor.org/stable/1312740.

Rastetter, E. B., G. I. Ågren, and G. R. Shaver. 1997. "Responses of N-Limited Ecosystems to Increased CO2: A Balanced-Nutrition, Coupled-Element-Cycles Model." *Ecological Applications* 7(2): 444–60. https://doi.org/10.1890/1051-0761(1997)007[0444:RONLET]2.0.CO;2.

Rastetter, E. B., G. W. Kling, G. R. Shaver, B. C. Crump, L. Gough, and K. L. Griffin. 2021. "Ecosystem Recovery from Disturbance Is Constrained by N Cycle Openness, Vegetation-Soil N Distribution, Form of N Losses, and the Balance between Vegetation and Soil-Microbial Processes." *Ecosystems* 24(3): 667–85. https://doi.org/10.1007/s10021-020-00542-3.

Rastetter, E. B., and B. L. Kwiatkowski. 2020. "An Approach to Modeling Resource Optimization for Substitutable and Interdependent Resources." *Ecological Modelling* 425: 109033. https://doi.org/10.1016/j.ecolmodel.2020.109033.

Rastetter, E., B. Kwiatkowski, D. Kicklighter, A. Barker Plotkin, H. Genet, J. Nippert, K. O'Keefe, et al. 2022b. "Ecosystem Responses to Changes in Climate and Carbon Dioxide in Twelve Mature Ecosystems Ranging from Prairie to Forest and from the Arctic to the Tropics ver 2." Environmental Data Initiative. https://doi.org/10.6073/pasta/7ca56dfbe6c9bedf5126e9ff7e66f28d.

Rastetter, E., B. Kwiatkowski, D. Kicklighter, A. Barker Plotkin, H. Genet, J. Nippert, K. O'Keefe, et al. 2022a. "Steady State Carbon, Nitrogen, Phosphorus, and Water Budgets for Twelve Mature Ecosystems Ranging from Prairie to Forest and from the Arctic to the Tropics ver 3." Environmental Data Initiative. https://doi.org/10.6073/pasta/b737b5f0855aa7afeda68764e77aec2a.

Rastetter, E. B., R. B. McKane, G. R. Shaver, and J. M. Melillo. 1992. "Changes in C Storage by Terrestrial Ecosystems: How CN Interactions Restrict Responses to CO_2 and Temperature." In *Natural Sinks of CO_2*, edited by J. Wisniewski and A. E. Lugo, 327–44. Dordrecht: Springer.

Rastetter, E. B., R. D. Yanai, R. Q. Thomas, M. A. Vadeboncoeur, T. J. Fahey, M. C. Fisk, B. L. Kwiatkowski, and S. P. Hamburg. 2013. "Recovery from Disturbance Requires Resynchronization of Ecosystem Nutrient Cycles." *Ecological Applications* 23(3): 621–42. https://doi.org/10.1890/12-0751.1.

Reilly, J., J. Melillo, Y. Cai, D. Kicklighter, A. Gurgel, S. Paltsev, T. Cronin, A. Sokolov, and A. Schlosser. 2012. "Using Land to Mitigate Climate Change: Hitting the Target, Recognizing the Trade-Offs." *Environmental Science & Technology* 46(11): 5672–9. https://doi.org/10.1021/es2034729.

Rollinson, C. R., Y. Liu, A. Raiho, D. J. P. Moore, J. McLachlan, D. A. Bishop, A. Dye, et al. 2017. "Emergent Climate and CO 2 Sensitivities of Net Primary Productivity in Ecosystem Models Do Not Agree with Empirical Data in Temperate Forests of Eastern North America." *Global Change Biology* 23(7): 2755–67. https://doi.org/10.1111/gcb.13626.

Shaver, G. R., A. E. Giblin, K. J. Nadelhoffer, K. K. Thieler, M. R. Downs, J. A. Laundre, and E. B. Rastetter. 2006. "Carbon Turnover in Alaskan Tundra Soils: Effects of Organic Matter Quality, Temperature, Moisture and Fertilizer." *Journal of Ecology* 94(4): 740–53. https://doi.org/10.1111/j.1365-2745.2006.01139.x.

Shaver, G. R., and S. Jonasson. 1999. "Response of Arctic Ecosystems to Climate Change: Results of Long-Term Field Experiments in Sweden and Alaska." *Polar Research* 18(2): 245–52. https://doi.org/10.1111/j.1751-8369.1999.tb00300.x.

Silva, L. C. R., and M. Anand. 2013. "Probing for the Influence of Atmospheric CO2 and Climate Change on Forest Ecosystems across Biomes." *Global Ecology and Biogeography* 22(1): 83–92. https://doi.org/10.1111/j.1466-8238.2012.00783.x.

Sokal, R. R., and F. J. Rohlf. 1995. Biometry: The Principles and Practice of Statistics in Biological Research., Third ed. New York: W. H. Freeman.

Thornton, P. E., S. C. Doney, K. Lindsay, J. K. Moore, N. Mahowald, J. T. Randerson, I. Fung, J.-F. Lamarque, J. J. Feddema, and Y.-H. Lee. 2009. "Carbon-Nitrogen Interactions Regulate Climate-Carbon Cycle Feedbacks: Results from an Atmosphere-Ocean General Circulation Model." *Biogeosciences* 6(10): 2099–120. https://doi.org/10.5194/bg-6-2099-2009.

Thum, T., S. Caldararu, J. Engel, M. Kern, M. Pallandt, R. Schnur, Y. Lin, and S. Zaehle. 2019. "A New Model of the Coupled Carbon, Nitrogen, and Phosphorus Cycles in the Terrestrial Biosphere (QUINCY v1. 0; Revision 1996)." *Geoscientific Model Development* 12(11): 4781–802. https://doi.org/10.5194/gmd-12-4781-2019.

Valipour, M., C. E. Johnson, J. J. Battles, J. L. Campbell, T. J. Fahey, H. Fakhraei, and C. T. Driscoll. 2021. "Simulation of the Effects of Forest Harvesting under Changing Climate to Inform Long-Term Sustainable Forest Management Using a Biogeochemical Model." *Science of the Total Environment* 767: 144881. https://doi.org/10.1016/j.scitotenv.2020.144881.

Wang, Y. P., R. M. Law, and B. Pak. 2010. "A Global Model of Carbon, Nitrogen and Phosphorus Cycles for the Terrestrial Biosphere." *Biogeosciences* 7(7): 2261–82. https://doi.org/10.5194/bg-7-2261-2010.

Wang, W. J., S. Ma, H. S. He, Z. Liu, F. R. Thompson, W. Jin, Z. F. Wu, et al. 2019. "Effects of Rising Atmospheric CO2, Climate Change, and Nitrogen Deposition on Aboveground Net Primary Production in a Temperate Forest." *Environmental Research Letters* 14(10): 104005. https://doi.org/10.1088/1748-9326/ab3178.

Wieder, W. R., C. C. Cleveland, W. K. Smith, and K. Todd-Brown. 2015. "Future Productivity and Carbon Storage Limited by Terrestrial Nutrient Availability." *Nature Geoscience* 8(6): 441–4. https://doi.org/10.1038/ngeo2413.

Wieder, W. R., J. F. Knowles, P. D. Blanken, S. C. Swenson, and K. N. Suding. 2017. "Ecosystem Function in Complex Mountain Terrain: Combining Models and Long-Term Observations to Advance Process-Based Understanding." *Journal of Geophysical Research: Biogeosciences* 122(4): 825–45. https://doi.org/10.1002/2016jg003704.

Wu, Z., E. Dai, W. Zhifeng, and M. Lin. 2019. "Future Forest Dynamics under Climate Change, Land Use Change, and Harvest in Subtropical Forests in Southern China." *Landscape Ecology* 34(4): 843–63. https://doi.org/10.1007/s10980-019-00809-8.

Xiao, W., X. Chen, X. Jing, and B. Zhu. 2018. "A Meta-Analysis of Soil Extracellular Enzyme Activities in Response to Global Change." *Soil Biology and Biochemistry* 123: 21–32. https://doi.org/10.1016/j.soilbio.2018.05.001.

Yang, G., Y. Peng, B. W. Abbott, C. Biasi, B. Wei, D. Zhang, J. Wang, et al. 2021. "Phosphorus Rather than Nitrogen Regulates Ecosystem Carbon Dynamics after Permafrost Thaw." *Global Change Biology* 27(22): 5818–30. https://doi.org/10.1111/GCB.15845.

Yang, X., and W. M. Post. 2011. "Phosphorus Transformations as a Function of Pedogenesis: A Synthesis of Soil Phosphorus Data Using Hedley Fractionation Method." *Biogeosciences* 8(10): 2907–16. https://doi.org/10.5194/bg-8-2907-2011.

Yang, X., D. M. Ricciuto, P. E. Thornton, X. Shi, X. Min, F. Hoffman, and R. J. Norby. 2019. "The Effects of Phosphorus Cycle Dynamics on Carbon Sources and Sinks in the Amazon Region: A Modeling Study Using ELM v1." *Journal of Geophysical Research: Biogeosciences* 124(12): 3686–98. https://doi.org/10.1029/2019JG005082.

Yuan, Z. Y., and H. Y. H. Chen. 2015. "Decoupling of Nitrogen and Phosphorus in Terrestrial Plants Associated with Global Changes." *Nature Climate Change* 5(5): 465–9. https://doi.org/10.1038/nclimate2549.

Zaehle, S., B. E. Medlyn, M. G. De Kauwe, A. P. Walker, M. C. Dietze, T. Hickler, Y. Luo, et al. 2014. "Evaluation of 11 Terrestrial Carbon–Nitrogen Cycle Models against Observations from Two Temperate F Ree-A Ir CO_2 E Nrichment Studies." *New Phytologist* 202(3): 803–22. https://doi.org/10.1111/nph.12697.

Zhu, Q., W. J. Riley, C. M. Iversen, and J. Kattge. 2020. "Assessing Impacts of Plant Stoichiometric Traits on Terrestrial Ecosystem Carbon Accumulation Using the E3SM Land Model." *Journal of Advances in Modeling Earth Systems* 12(4): e2019MS001841. https://doi.org/10.1029/2019MS001841.

SUPPORTING INFORMATION

Additional supporting information can be found online in the Supporting Information section at the end of this article.

How to cite this article: Rastetter, Edward B., Bonnie L. Kwiatkowski, David W. Kicklighter, Audrey Barker Plotkin, Helene Genet, Jesse B. Nippert, Kimberly O'Keefe, et al. 2022. "N and P Constrain C in Ecosystems under Climate Change: Role of Nutrient Redistribution, Accumulation, and Stoichiometry." *Ecological Applications* e2684. https://doi.org/10.1002/eap.2684